

POLITECNICO DI MILANO

**Scuola di Ingegneria Industriale e dell'Informazione
Dipartimento di Elettronica, Informazione e Bioingegneria**

Corso di Laurea Magistrale in Ingegneria Biomedica



**DESIGN OPTIMIZATION OF A PASSIVE SOFT
ROBOTIC DEVICE FOR NEUROREHABILITATION**

Relatore: Prof. Elena De Momi
Correlatore: Prof. James L. Patton

Tesi di Laurea di:
Tommaso Carella Matr. 877966

Anno Accademico 2018-2019

*To my Grandfather, Cesare, and my Aunt, Giuliana,
who are no more among us.
I know that even where you are now you are still very proud of me.*

Acknowledgements

First and foremost, I would like to express my most sincere gratitude to Prof. Elena De Momi, whose guidance and suggestions made this work possible.

Thanks to all my *Gente Malata* friends: you are my second family and my life would be boring without you! With your support you all gave me the strength to go on on this difficult path. Please, never change!

Moreover, I want to thank Baro and the other friends from Politecnico for sharing never-ending classes with me.

Moreover, thanks to all the people that were with me in Chicago, you made that experience the best possible!

The most important thanks to Giulia, I would not have been here without your help and your support; I know I am an unaffectionate person the most of the time, but I want to say that sharing with you this journey made it the best experience of my life.

Thanks to all my grandparents, Enrico, Raffaella and Anna for always supporting me and taking care of me, to my uncle, Chicco, and my aunt, Valentina, for helping me financially and for being always present. Moreover, a special mention also to the *Tradatesi* and to the growing Grazioli family.

Last but not least, thanks from the bottom of my heart to my parents, Fabio and Fabrizia; you made me the person I am now and the one I will become and I would never be able to express the gratitude I feel. Thank you, also, to my sisters Caterina, Benedetta and Sonya and my brother, Simone, for making my everyday life so special and full of meaning.

Milano, Aprile 2019

T. C.

Contents

Abstract	I
Sommario	II
1 Introduction	2
1.1 Motivation	2
1.1.1 Stroke survivors: a growing population	2
1.1.2 Robotic rehabilitation	3
1.2 Prior Studies	3
1.2.1 MARIONET: first model	3
1.2.2 MARIONET: at-home rehabilitation device	4
1.2.3 Gravity compensation	5
1.3 Thesis	6
2 Methods	7
2.1 MARIONET revisited: basic concepts	7
2.1.1 Geometry	8
2.1.2 Single component torque profile	8
2.2 Stacking MARIONETs	11
2.3 Two-joints MARIONET	12
2.4 Empirical optimization	14
2.4.1 Code description	14
2.5 Gravity compensation	18
2.6 Experimental setup	24
2.6.1 Protocol	24
2.6.2 Data analysis	24
3 Results and Discussion	25
3.1 Optimization results	25
3.1.1 Simulation with two Parameters: <i>Radius</i> and <i>Angle ϑ</i>	25
3.1.2 Simulation with three Parameters: <i>Radius</i> , <i>Angle ϑ</i> and <i>Stiffness k</i>	29
3.1.3 How many stacked MARIONETs?	31
3.1.4 Problems connected to random initialization	33
3.2 Gravity compensation results	35
3.2.1 One-joint solution	35
3.2.2 A MARIONET crossing two joints	41
3.2.3 A complete MARIONET	44

4 Conclusions and future development	46
Acronimi	49
Bibliography	49

List of Figures

1.1	Torque controlled through changes in the moment arm.	4
2.1	Basic concept of the MARIONET applied to the fore arm: R is the distance between the CoR and the point where the spring is attached, ϑ the angle between the horizontal and R , L is the arm length and φ is the angle between the horizontal and the arm.	7
2.2	Diagram of the MARIONET.	8
2.3	Torque generated by a single MARIONET in the range $[0, 2\pi]$. This makes a nearly sinusoidal basis function that can be shaped and combined with others.	9
2.4	Torque generated by different single MARIONETs in the range $[0, 2\pi]$; varying parameters allows one to have different sinusoids: for the <i>blue</i> profile $\vartheta = \frac{\pi}{3}$ and $R = 0.1m$, for the <i>red</i> one $\vartheta = \frac{2\pi}{3}$ and $R = 0.1m$ and for the <i>green</i> one $\vartheta = \frac{2\pi}{3}$ and $R = 0.05m$	10
2.5	Concept of a 3-stacked elements configuration.	11
2.6	Overall torque generated by the sum of MARIONETs.	12
2.7	Diagram of the two-joints MARIONET.	12
2.8	Flow chart of the developed MATLAB code: here are all the step implemented in order to find the optimal solution.	14
2.9	Free-body diagram used to calculate the torque needed for gravity compensation.	18
2.10	Free-body diagram that represents the torques as a force (F), as calculated through 2.18.	20
2.11	Vector field: each <i>red</i> arrow is the force at a certain shoulder-elbow angle couple able to compensate weight.	20
2.12	Elbow and Shoulder torque needed in order to compensate for gravity for fixed φ_1 and φ_2 respectively.	21
2.13	Target torque at the shoulder for the two-joints version.	22
3.1	Top: in <i>blue</i> the torque generated by 5 MARIONETs, in <i>red</i> the target one. Bottom: the error (in <i>green</i>), calculated as the difference between the red and blue profiles, and the average error (<i>black</i> line); moreover, some information about the error are shown.	26
3.2	How the MARIONETs are arranged in the space: in <i>blue</i> is the parameter R and in <i>green</i> is the spring.	27
3.3	Top: in <i>blue</i> the overall torque generated by 5 MARIONETs is represented, while in <i>cyan</i> each single component is pictured.	27

3.4	Results obtained with a smoother target torque. <i>Top</i> : the two torque fields were almost completely overlapped. <i>Bottom</i> : A smoother target resulted in smaller errors.	28
3.5	Top: in <i>blue</i> the torque generated by 5 MARIONETs, each tuned according to three parameters R , ϑ and k , in <i>red</i> the target one. Bottom: the error (in <i>green</i>), calculated as the difference between the red and blue profiles, and the average error (<i>black</i> line); moreover, some information about the error is shown.	29
3.6	Trend of the average error with respect to the the number of stacked elements: each point represents the average absolute error as obtained with a certain number of stacked elements.	31
3.7	Flow chart of the developed algorithm.	33
3.8	Average error for each iteration.	34
3.9	Comparison of the result of two different output of the algorithm. . . .	35
3.10	Elbow torques that are approximated in the best and worst way, respectively.	37
3.11	Shoulder torques that are approximated in the best and worst way, respectively.	39
3.12	Vector field that we want to achieve (in <i>red</i>) and optimal field obtained with the algorithm (in <i>black</i>).	40
3.13	Arrangement of a one-joint and two-joint MARIONETs.	41
3.14	Attempts to cancel gravity: the large amount of error suggests that a two-joint MARIONET by itself cannot provide adequate gravity cancellation (color convention match previous figures).	42
3.15	Vector field that we want to achieve (in <i>red</i>) and optimal field (in <i>black</i>) as obtained through the two-joints version of the algorithm; adequate gravity cancellation appears to be difficult with this mechanism by itself.	43
3.16	Final attempt to cancel gravity: the mixed device seems able to compensate for arm weight (color convention match previous figures).	44
3.17	Vector field that we want to achieve (in <i>red</i>) and optimal field (in <i>black</i>) as obtained through the mixed version of the algorithm; adequate gravity is achievable with this mechanism.	45
4.1	A possible design of the MARIONET.	47
4.2	The first prototype of the MARIONET is being developed at the Shirley Ryan Ability Lab; in this picture it is possible to see the complete device with the mixed configurations.	48

List of Tables

3.1	OPTIMAL PARAMETERS FOR EACH SINGLE COMPONENT. . .	26
3.2	OPTIMAL PARAMETERS FOR EACH SINGLE COMPONENT. . .	29
3.3	AVERAGE ERROR [Nm] WITH RESPECT TO THE NUMBER OF STACKED ELEMENTS.	31
3.4	AVERAGE ERROR [Nm], AVERAGE ERROR [%] AND R^2 FOR EACH PROFILE FOR ELBOW TORQUE.	36
3.5	OPTIMAL PARAMETERS FOR GRAVITY COMPENSATION AT THE ELBOW JOINT.	36
3.6	AVERAGE ERROR [Nm] AND AVERAGE ERROR [%] FOR EACH PROFILE FOR SHOULDER TORQUE.	38
3.7	OPTIMAL PARAMETERS FOR GRAVITY COMPENSATION AT THE SHOULDER JOINT.	38

Abstract

Nowadays, more and more people who underwent brain damages (i.e. after a stroke) are in need for rehabilitation, a necessary tool for restoration of their functional capacity. In order to meet this compelling need, robotic devices are employed not only to facilitate and accelerate rehabilitation, but also to achieve better results where previous therapies failed.

The MARIONET¹ is a simple mechanism able to exert customized torque profiles to the patient's limbs by adjusting the moment arm in order to obtain torque. Here, the MARIONET is expanded so as to obtain a portable system, completely passive and customizable to the needs and disabilities of the patient patient. Not only this device is thought to fit into a large variety of anthropometric dimensions, but also to achieve different tasks, such as assistance, error augmentation and gravity compensation.

The MARIONET, thanks to its design, is able to exert a sinusoidal torque field; so, the possibility to "stack" a certain number of devices is taken into account so as to obtain more complex torque profiles; this concept is similar to a truncated Fourier Transform, with each mechanism acting as a basis function.

The goal of this work is to optimize the design of the MARIONET by computing a set of optimal parameters which, in turn, could be used to customize the device according to the patient's need.

The algorithm that was used to optimize the design was tested, in the end, so as to adjust the MARIONET in a way to achieve gravity compensation of the arm, a process that helps the patient during its rehabilitation path by balancing the weight of the arm itself.

Keywords: Rehabilitation robotics, Neurorehabilitation

¹Moment arm Adjustment for Remote Induction Of Net Effective Torque

Sommario

Oggi giorno, sempre più persone che hanno subito danni cerebrali (i.e. ictus) necessitano di riabilitazione, uno strumento necessario per il paziente per recuperare le proprie funzionalità perdute. L'utilizzo di dispositivi robotici permette di venire incontro a questo impellente bisogno, non solo in modo da facilitare ed accelerare la riabilitazione del paziente ma anche per poter ottenere migliori risultati là dove le tecniche classiche falliscono.

MARIONET è un semplice meccanismo in grado di produrre momenti personalizzati al paziente aggiustando il braccio del momento. In questo lavoro il concetto di MARIONET viene allargato in modo da ottenere un sistema portatile, completamente passivo e personalizzabile a seconda dei bisogni del paziente; non solo il dispositivo è in grado di adattarsi a diverse misure antropometriche, ma anche essere utilizzato per diversi compiti, come assistenza, aumento dell'errore e compensazione di gravità.

Poiché MARIONET è in grado di esercitare un momento di tipo sinusoidale grazie al suo design, viene presa in considerazione la possibilità di "impilare" un certo numero di dispositivi in modo da ottenere momenti via via più complessi; il concetto è simile ad una Trasformata di Fourier troncata, con ogni meccanismo che agisce come una funzione di base.

L'obiettivo di questo lavoro è l'ottimizzazione del design di MARIONET attraverso il calcolo di una serie di parametri; in questo modo è possibile adattare MARIONET ai diversi bisogni di ogni paziente.

Infine, l'algoritmo utilizzato per l'ottimizzazione è testato, in particolare, in modo da simulare un dispositivo che sia in grado di compensare totalmente il peso del braccio del paziente, una tecnica che permette di aiutarlo nel suo percorso di riabilitazione.

Parole chiave: Riabilitazione robotica, Neuroriabilitazione

Chapter 1

Introduction

1.1 Motivation

1.1.1 Stroke survivors: a growing population

Stroke is the leading cause worldwide for what concerns long-term disability; in fact, one in 6 people in the world will experience stroke and ≈ 750000 people in the US are affected each year [1], with survival rate of the 82% [2]. Moreover, more than the 50% of the survivors will experience lasting disabilities [3] such as sensation loss, spasticity, imbalance strength, jerkiness, muscle coupling, poor planing and motion inaccuracies, leading to the inability to perform the so-called ADLs¹, a set of functional movements such as routine tasks of personal care, feeding or communicating [4]. Because of the aging of the population, the number of cases is destined to rise dramatically in the next years; recent statistics, in fact point out that only 10% of stroke patient are between the age of 18 and 50 [5]. Stroke generates an estimated expense of 33 billion dollars connected to not only the health care and lost days at work [1]; moreover, it results in a decreased quality of life not only for the patients and their families, but also for the caregivers [6] [7] [8] [9].

For this growing population, rehabilitation is the process that aims to restore the maximum functional capacity possible and it is the only way for a patient, who presents residual disability, to improve his condition. Therapy should start at an early stage or, otherwise, the chances to obtain an acceptable recovery are reduced [10]. However, researchers have indicated that, even more than 6 months after the stroke (in the phase that is called chronic stage), there is the possibility to further motor recovery [11] [12], but, since insurances providers do not usually cover chronic patients' therapies and for the therapists working with them, the needed help to recover should be found somewhere else.

¹Activities of Daily Living

1.1.2 Robotic rehabilitation

In this context, machine-assisted therapy has been proven to be reasonable for enhancing physical outcomes for patients who suffered from neurological disabilities. In general, past research has been focusing on active robotic devices, in which the patient is physically guided by the robot itself in order to accomplish a specific movement and the therapist acts as a simple bystander. Some of these previous devices are the MIME², a 6 DoF³ end effector which applies forces in a certain direction so as to achieve the desired movement [13], and the InMotion2 (MIT MANUS), a 2 DoF robot that shows three different modalities for the user, among which the totally assisted movement procedure, in which the arm is moved passively [14].

Although devices such as the InMotion2 were shown to motivate patients to practice and to have a positive therapeutic advantage, subjects do not improve if the technology dominates movements [15] [16]; the main reason, as many researchers pointed out, is that, being guided completely by a robot, a patient can become lazy [17] [18]. Moreover, robotic guidance machines are still expensive (for example, InMotion2 costs ≈ 100000 \$). Finally, since stroke varies widely in effects and severity, it is problematic to treat patients in the same way.

From these problems the need to advance devices arises. They should be lightweight, low-cost, easy to operate and customizable. Moreover, in recent years simple exoskeletons for assistance, therapy and motor control have been developed: they involved passive elements, such as springs, which are able to generate desired torques [19] [20].

1.2 Prior Studies

One attempt to find a solution to the aforementioned issues was done in our group with the MARIONET [21] [22], a cable-driven device, which is able to deliver torque to a joint. This kind of design aims at controlling the generated torque through changes in the moment arm (1.1), whereas in most of the previous mechanisms, such as the String-Man [23], the moment exerted is a function of the cable tension.

1.2.1 MARIONET: first model

The first prototype of the MARIONET was part of the family of the so-called SEA⁴ mechanisms, which are formed by an elastic element in series with an actuator. The advantage of this kind of approach is that torque ripple, undesired errors and backlash are dampened, though some position accuracy and bandwidth are sacrificed as a

²Mirror-Image Motion Enabler

³Degrees of Freedom

⁴Series Elastic Actuators

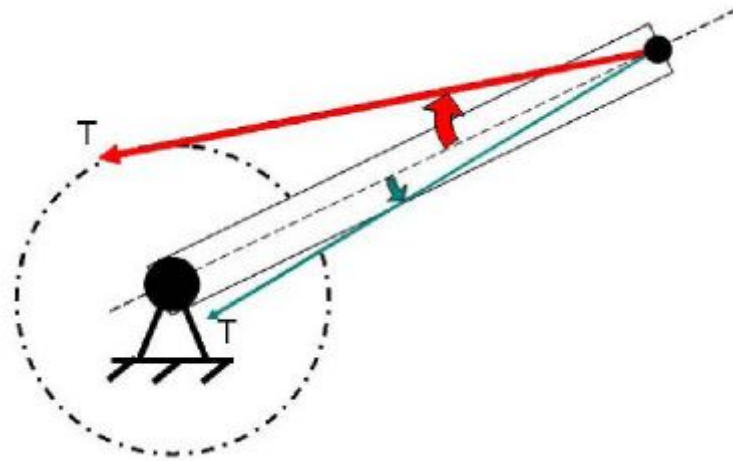


Figure 1.1: Torque controlled through changes in the moment arm: being equal the stiffness, a longer arm results in a higher torque (as pictured by the thicker *red* arrow); the *blue* one shows that a smaller arm produces a lower moment [22].

result; the fundamental compliance of the SEAs is highly suitable for human–robot interactions [24]. The mechanism consisted of a rotator, actively controlled by a motor, and a passive link; a second motor worked as a tensioner. Despite not presenting springy components, the MARIONET behaved exactly as a SEA, creating conservative force field generated via the tensioner. Although the system presented mechanical issues, connected mainly to friction, it managed to deliver torque to the desired joint with the convenience of remote actuation and independent control on equilibrium and compliance [21]. However, this version of the device was still a non–wearable, ”heavy duty” robot.

1.2.2 MARIONET: at–home rehabilitation device

Whereas the first model was thought as a one–joint device, in the second generation the concept of the MARIONET was expanded so as to achieve an inexpensive two–joint machine for at–home rehabilitation [22]. Since it was developed as a tool for private use, the first issue to address was the user’s safety, resulting in a device that presented low inertia and a low impedance with the interface, thanks to the use of SEAs; moreover, the actuator, being the heaviest part of the overall machine, was moved to the base of the device.

The design of this second prototype was divided into four different parts:

1. *Design for Function:* the two–joints system had to be a Manipulandum for upper extremities, highly customizable, so as to fit several users, and safe; furthermore, it had to be lightweight, inexpensive and mobile.
2. *Design with Cables:* the use of cables has some drawbacks, like the fact that they can wear out; therefore, the arrangement of the MARIONET aimed at avoiding

process such as rope twisting, sharp augment in load, wrapping, etc.

3. *Design for Safety*: safety of the patient was the main concern; many possible failures modes were taken into account when designing the system, such as cable failure, electrical faults, etc., addressing each of them (cable guards, mechanical stops).
4. *Design for Control*: the MARIONET was controlled by four inputs: the position of the rotators (for every joint) and the motors acting as tensioners.

The most interesting aspect is that the device no longer needed rigid links, but, instead, the patient's arm itself was sufficient as a stiff element; moreover, since the MARIONET did not use elastic elements, cushioning came from the natural damping of the human arm, which showed to be more than enough to avoid instability [22]. Finally, it is important to point out that the system was suitable to accomplish gravity compensation (section 1.2.3) and to exert both assistive and error enhancing forces, the latter being a new rehabilitation technique that will be addressed in section ??.

1.2.3 Gravity compensation

In order to improve rehabilitation, many scientist focused on *gravity compensation* for the upper limbs, considering a possible involvement of robots. The aim is to compensate for the weight of the patient's arm, so as to augment their active range of motion [25]; in fact, as several studies showed, the working area of patients increased immediately during reaching tasks performed while providing gravity compensation with respect to unsupported movements [26]. In order to implement this method, the torque generated by the arm weight at each joint is calculated and compensated through the robot. One attempt to achieve gravity compensation was made by Sanchez et al. with the T-WREX⁵ [27] a passive, backdriveable, five DoF mechanism that counterbalanced the arm weight using elastic bands. This device was thought for at-home rehabilitation, thus presenting important safety constraints such as not generating power and the incapability to move on its own. Researchers demonstrated the ability to allow a larger range of motion, helping patients in performing ADLs. However, on the other hand, the system resulted in a more expensive device with respect to other devices on the market, and, moreover, it is only able to implement fixed levels of gravity support dependent on the number of elastic bands that are used.

Therefore, there is the need for new rehabilitation tools that have to be customizable, lightweight and cheap. Moreover, these new systems should be able to exert torque without being actuated so as to avoid having a power source or electrical parts in order to be safe.

⁵Therapy Wilmington Robotic Exoskeleton

1.3 Thesis

Accordingly, this work aims at designing a new version of the MARIONET, a completely passive one, simplifying the actuators in order to use only elastic elements (such as diagonal springs), lightweight, versatile and cheap. Furthermore, this device should be highly customizable to match the characteristics and specific motor deficit of the patient (length of the arm, torque profile needed, etc.) and should be quickly assembled by a therapist.

Next, at a later time, we will explore the possibility to stack a certain number of MARIONETs so as to achieve a more complex torque profile; in fact, each MARIONET behaves as a basis function taking advantage of its intrinsic sinusoidal nature. The device could be used to fill in the gap of motor ability or to achieve *gravity compensation*. The main part of the work concentrates on computationally finding a set of optimal parameters for the stacked device, customizing it for the user through an optimization problem in MATLAB. Moreover, a two-joint MARIONET is studied, and the gravity compensation problem is addressed and solved to counterbalance the weight of the arm in the overall workspace. In Chapter 2 the methods will be addressed, while in Chapter 3 results will be shown and discussed; finally, in Chapter 4 conclusions on the work will be drawn.

Chapter 2

Methods

2.1 MARIONET revisited: basic concepts

As stated in section 1.3, the new concept of the MARIONET involves a completely passive tool, formed by a pegboard to which a springy element is attached; there is no rigid link, since this part is substituted by the arm itself (2.1).

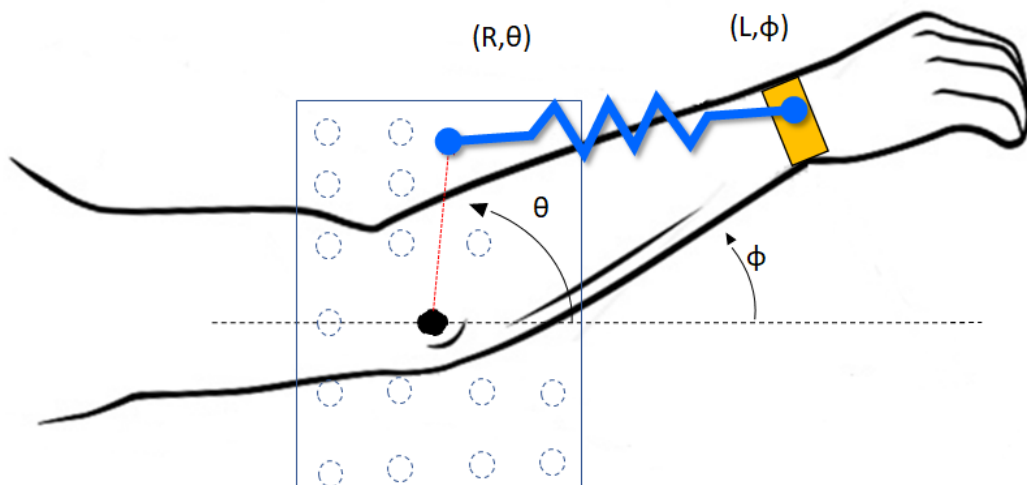


Figure 2.1: Basic concept of the MARIONET applied to the fore arm: R is the distance between the CoR and the point where the spring is attached, ϑ the angle between the horizontal and R , L is the arm length and φ is the angle between the horizontal and the arm.

2.1.1 Geometry

The geometry underlying the device is quite simple and is shown in 2.2. Being R (in *yellow*) the distance between the CoR¹ (*green*) and the point where the spring is attached, ϑ the angle between R and the horizontal (dashed line), L (*black*) the length of the arm link and φ the one between L and the horizontal, the length of the spring L_s (*blue*) is:

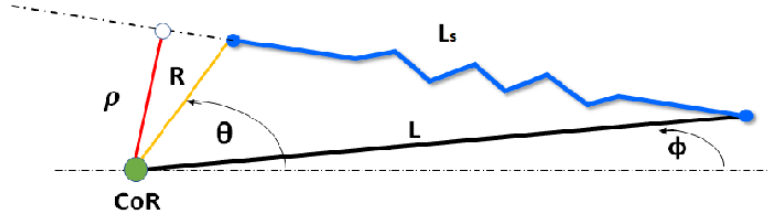


Figure 2.2: Diagram of the MARIONET.

$$L_s(\varphi) = \sqrt{R^2 + L^2 - 2RL \cos(\vartheta - \varphi)}. \quad (2.1)$$

In order to calculate the torque (τ) exerted by the device, the moment arm (ρ , *red* in 2.2), which is a function of φ , since it varies as the angle changes:

$$\rho(\varphi) = \frac{RL \sin(\vartheta - \varphi)}{L_s}. \quad (2.2)$$

Therefore is possible to calculate the torque as:

$$\tau(\varphi) = F_s \times \rho, \quad (2.3)$$

where F_s is the force calculated through Hook's Law, being k the stiffness of the spring and Δx the displacement of the elastic element, as:

$$F_s = -k\Delta x. \quad (2.4)$$

2.1.2 Single component torque profile

Fig. 2.3 shows the torque generated by a single MARIONET, as calculated using Eq.2.1–2.4, with $\vartheta = \frac{\pi}{3}$, $R = 0.1m$, the rest length of the spring $L_R = 0.1m$, the length of the fore arm $L = 0.26m$ and the stiffness $k = 250 \frac{N}{m}$; its sinusoidal nature makes it suitable to act as a basis function and, so, a series of stacked elements can be used to achieve more complex torque shapes.

¹Center of Rotation

By varying only two parameters (R, ϑ), is it possible to achieve very different characteristics of these sinusoids, as displayed in 2.4: the *blue* shape having the same parameters as before, the *red* one has $\vartheta = \frac{2\pi}{3}$ and same R , while the *green* one has $R = 0.05m$ and same ϑ .

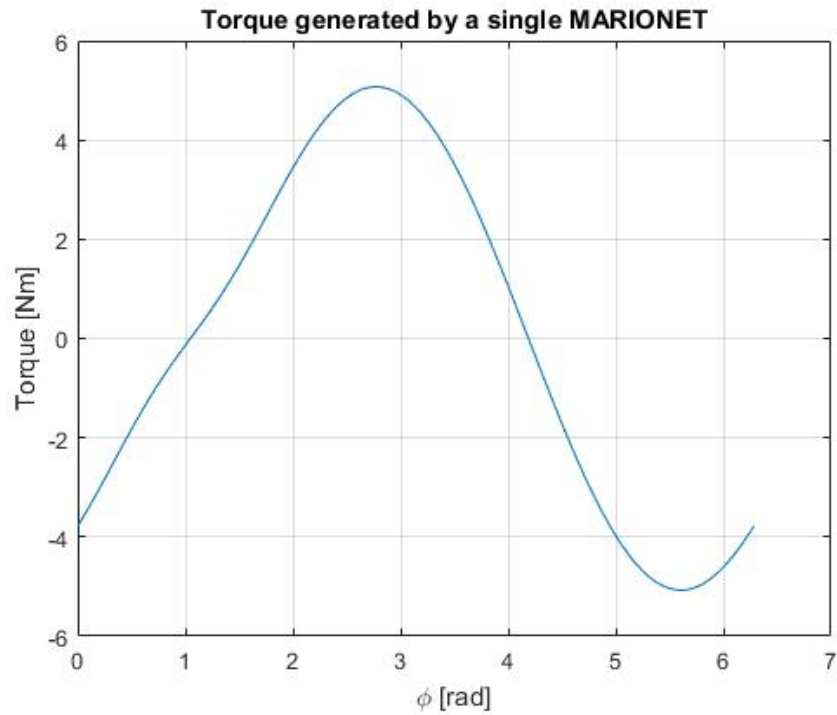


Figure 2.3: Torque generated by a single MARIONET in the range $[0, 2\pi]$. This makes a nearly sinusoidal basis function that can be shaped and combined with others.

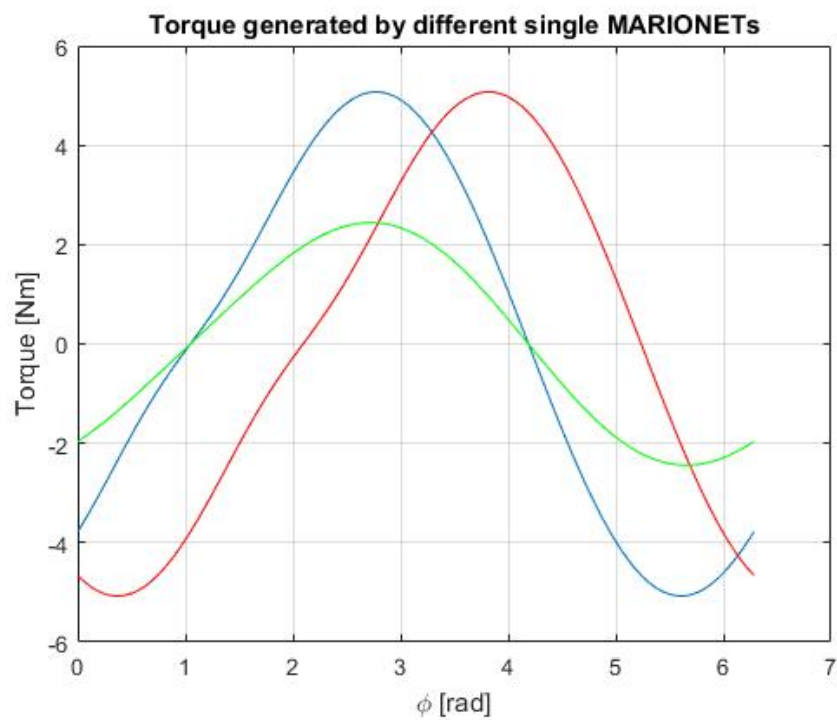


Figure 2.4: Torque generated by different single MARIONETs in the range $[0, 2\pi]$; varying parameters allows one to have different sinusoids: for the *blue* profile $\vartheta = \frac{\pi}{3}$ and $R = 0.1m$, for the *red* one $\vartheta = \frac{2\pi}{3}$ and $R = 0.1m$ and for the *green* one $\vartheta = \frac{2\pi}{3}$ and $R = 0.05m$.

2.2 Stacking MARIONETs

As previously noted, stacking more and more elements can lead to the generation of complicated torque fields. In 2.5, one possible solution for a multi-stacked elements configuration is shown.



Figure 2.5: Concept of a 3-stacked elements configuration.

The total torque generated by the overall device is given by the sum of the moments generated by each one of the n single elements:

$$\tau_{tot} = \tau_1 + \tau_2 + \dots + \tau_i + \dots + \tau_n \quad (2.5)$$

2.6 shows the torque generated by three different MARIONETs (in *black*); as previously stated, a unique torque profile can be obtained, so as to achieve a specific task.

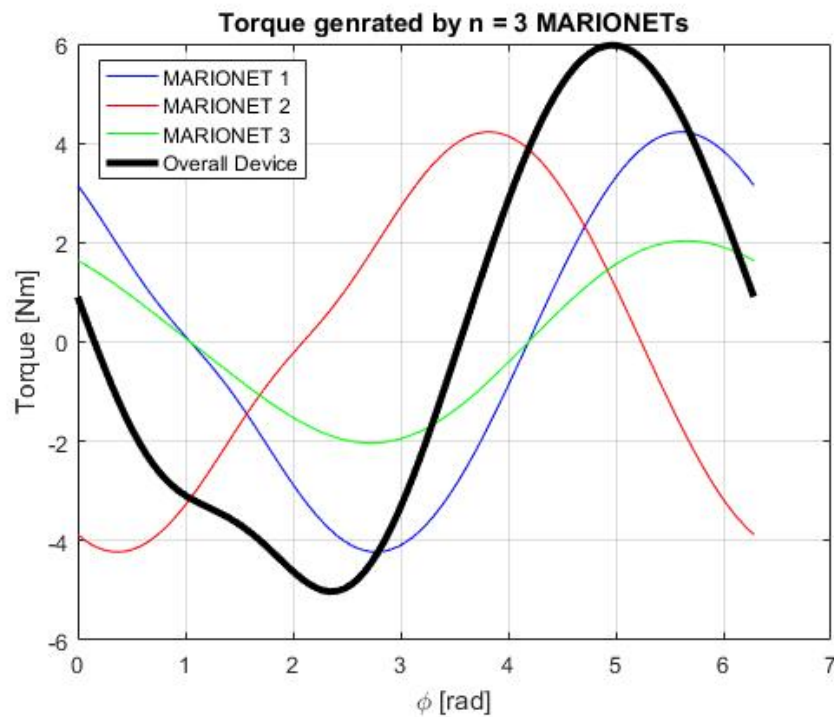


Figure 2.6: Overall torque generated by the sum of MARIONETs.

2.3 Two-joints MARIONET

An additional version of the MARIONET can be conceived linking directly the shoulder and the wrist through a spring, therefore obtaining a two-joints device. The scheme of the mechanism is reported in 2.7.

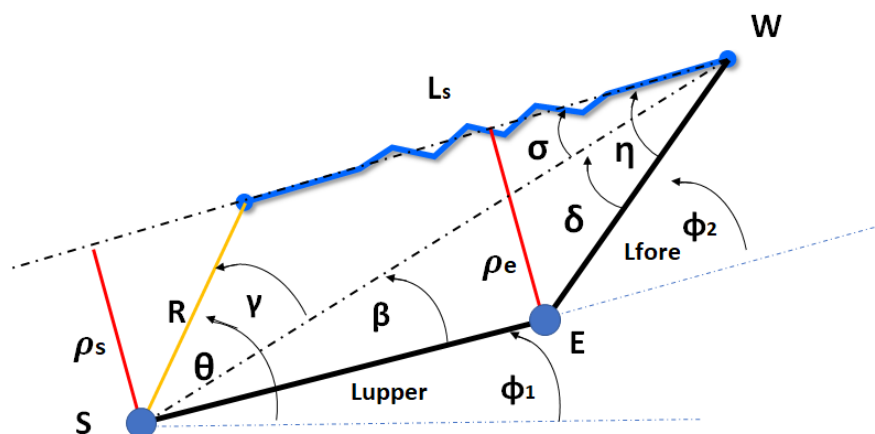


Figure 2.7: Diagram of the two-joints MARIONET.

First of all, the length of the spring L_s is calculated as:

$$L_s = \sqrt{\left(\frac{L_{fore} \sin(\varphi_2)}{\sin(\beta)}\right)^2 + R^2} - \left(\frac{L_{fore} \sin(\varphi_2)}{\sin(\beta)}\right) R \cos(\gamma), \quad (2.6)$$

where $\gamma = \vartheta - \beta - \varphi_1$ and β represents the angle between L_{upper} and the diagonal of the quadrilateral composed by L_{upper} , L_{fore} , L_s and R (*black* dotted line) and is calculated using the *atan2* MATLAB function.

Then, the moment arm at the shoulder joint ρ_s is calculated:

$$\rho_s = \frac{\left(\frac{L_{fore} \sin(\varphi_2)}{\sin(\beta)}\right) R \sin(\gamma)}{L_s}. \quad (2.7)$$

On the other hand, the moment arm at the elbow ρ_e is computed as:

$$\rho_e = L_{fore} \sin(\eta), \quad (2.8)$$

where $\eta = \delta + \sigma$, which are defined as:

$$\delta = \arcsin\left(\frac{L_{upper} \sin(\beta)}{L_{fore}}\right), \quad (2.9)$$

$$\sigma = \arcsin\left(\frac{R \sin(\gamma)}{L_s}\right), \quad (2.10)$$

Knowing ρ_s and ρ_e , the torques can be calculated using 2.3.

2.4 Empirical optimization

Now that the geometrical basis are set, we aim at replicating every torque needed by a certain patient for rehabilitation purposes. Therefore, each MARIONET has to be tuned according to certain parameters that we are determined to find through the solution of an optimization problem; the algorithm, which will be explained in the next paragraphs, can be set to find two or three *optimal parameters* for each element. Of course, the higher the number of stacked MARIONETs and, as a consequence, the higher the number of parameters to be found, the higher the computational cost and the time spent processing.

2.4.1 Code description

2.8 shows the flow chart of the MATLAB code that was developed in order to find the optimal parameters.

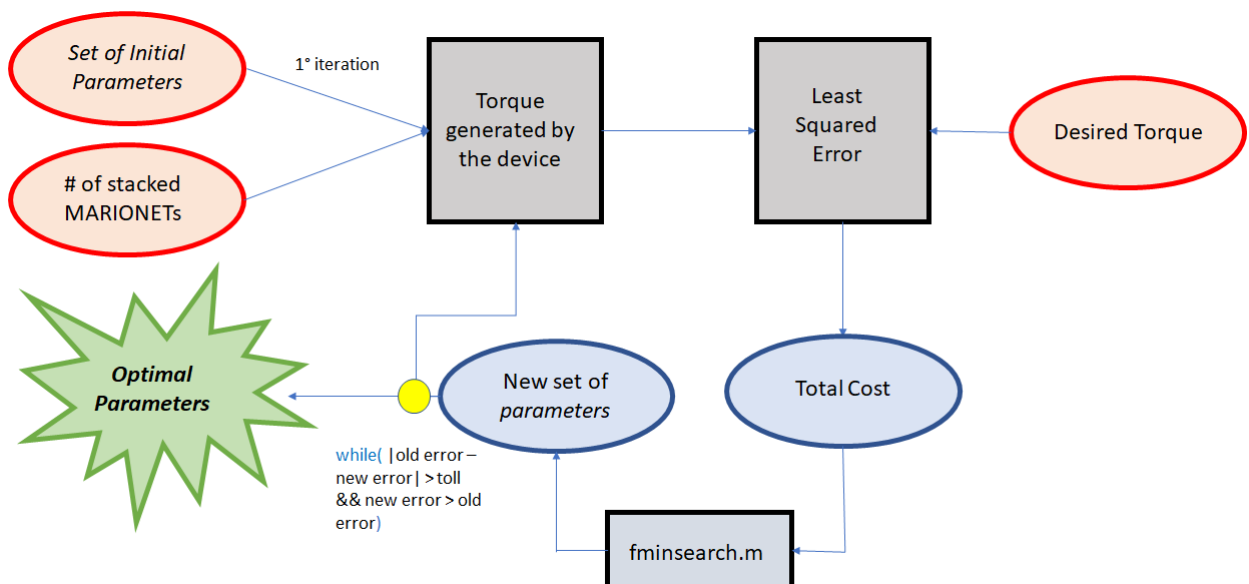


Figure 2.8: Flow chart of the developed MATLAB code: here are all the step implemented in order to find the optimal solution.

Inputs

There are three main *inputs* to the function (*red ovals*):

- *Number of stacked MARIONETs (N)*: the number of different elements that we want to combine in order to obtain the desired torque.
- *Set of initials parameters*: Being M the number of parameters for each element, a $M \times N$ vector is created; this vector is thus filled in with random numbers thanks to the *rand* function.
- *Desired torque*: The torque profile the patient needs for rehabilitation, as chosen by therapist or physician.

The initial overall torque (τ_{tot}) is calculated by using 2.3 with the starting random parameters for each MARIONET and by summing all the obtained moments as in 2.5.

Parameters

The two main parameters that the algorithm aims to find are R and ϑ (as represented in 2.1); the former is the distance between the CoR and the point on the pegboard where the spring is attached, while the latter is the angle between the horizontal line and R . Moreover, as pointed out before, a third parameter can be addressed: the stiffness of the elastic element k .

The first two parameters have an impact on the length of the moment arm (as expressed by 2.2), while the third one acts on the force exerted by the spring.

Cost calculation

The chosen cost function (Eq. 2.11) for the optimization algorithm is the *Least Squared Error*, as defined by:

$$Cost = \sum_1^n (\tau_{tot} - Desired\ Torque)^2, \quad (2.11)$$

being n the length of the *Desired Torque* vector. Furthermore, since the device should be built for the patient to be comfortable, some restriction to the parameters are set. These were employed as regularization terms, or soft constraints. Of course, the *Radius (R)* can not be negative and, in addition, its length its expected to be no longer than $0.1m$, since we want the patient to feel comfortable while wearing the device and a big mechanism would not accomplish such a requirement. For any $R < 0m$ and $R > 0.1m$ a *penalty function* was added, increasing the overall total cost. Moreover, some constraints are also applied to the stiffness of the elastic elements, when considered as a parameter in the optimization process; therefore, the cost increases when the *stiffness (k)* is $k < 0$ or

$k > 1000$. For both R and k , the cost was augmented by summing a penalty parameter multiplied by a factor measuring the violation of the constraints:

$$\text{PenaltyFunction} = |\text{Param} - \text{Param}_0|^3 \times 10^{15}, \quad (2.12)$$

where the variable Param is the parameter under review and Param_0 is the inferior or superior limit for the parameter itself.

On the other hand, no penalty is needed for ϑ , since this angle is used in a periodic function and, thus, the value can be taken in the period $[0, 2\pi]$.

fminsearch.m

This function, that is part of the *Optimization Toolbox* on MATLAB, is able to solve nonlinear problems using a derivative-free method; it aims at minimizing a given function, that, in this case, is the total cost as defined in section 2.4.1. Therefore, it is able to find the optimal parameters that correspond to a minimum [28]. The options were changed so as to have the highest number of iteration and evaluation of the function possible. Eventually, the output of this function is a new set of parameters, with which the new MARIONET torque is calculated.

Avoiding local minima

One iteration of the code is not enough to obtain satisfying outcomes, so an outer *while* loop is added. This is to assure that a more global optima is found. The *while* loop presents two main conditions and a third optional one:

- $|\text{meanError}_i - \text{meanError}_{i-1}| > \text{toll}$: if at the i^{th} step, the difference between the average error at i^{th} and $i - 1^{\text{th}}$ is bigger than a certain tolerance (*toll*, to be decided), then loop is repeated; the average error is calculated as the mean of the difference between the MARIONET torque and the desired one.
- $\text{meanError}_i > \text{meanError}_{i-1}$ if the mean error calculated at the i^{th} step is bigger than the error at the previous one, then the loop continues.

In order to leave the *while* loop, these two conditions must be false at the same time (logical OR); moreover, a third one can be added:

- $\text{number of iterations} > \text{MaxIter}$: this condition is added to avoid the code to get stuck; so, when the number of iterations i is bigger than a certain predetermined threshold (*MaxIter*), the *while* loop is left (being this condition linked with a logical AND to the previous two).

Optimal Parameters

When the *while* loop terminates, this means that the global *optimal parameters* have been found. These can be used to tune the different MARIONETs that are included in the device so as to achieve the torque needed by the patient.

2.5 Gravity compensation

In order to achieve gravity compensation, as defined in section 1.2.3, the first step is to find the torques needed to balance the moment generated by the arm weight; to do so, the free-body diagram of the human arm is studied. These torques are calculated under the condition of static equilibrium; moreover, the problem was simplified applying the weights of each part composing the arm at the middle point of each link, while the weight of the hand was applied at the wrist joint. 2.9 shows the free-body diagram taken as a reference: φ_1 is the angle between the horizontal line and the SE segment, φ_2 the one between SE and EW links, τ_s and τ_e the torques to be found at shoulder and elbow joint respectively; in addition, the aforementioned weights are shown.

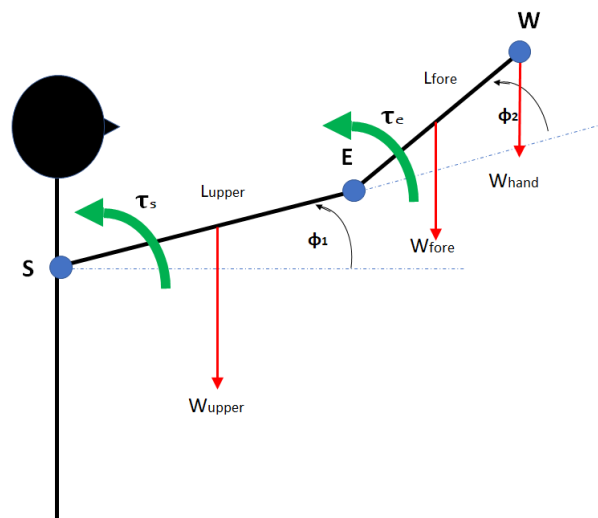


Figure 2.9: Free-body diagram used to calculate the torque needed for gravity compensation.

First of all, the mass of different parts of the arm is calculated as related to the TBM², as suggested by De Leva [29], and multiplied by the gravity acceleration ($g = 9.81 \frac{m}{s^2}$):

- *Upper arm weight:*

$$W_{upper} = 2.71\% \times TBM \times g. \quad (2.13)$$

- *Fore arm weight:*

$$W_{fore} = 1.62\% \times TBM \times g. \quad (2.14)$$

- *Hand weight:*

$$W_{hand} = 0.61\% \times TBM \times g. \quad (2.15)$$

Solving the static problem as depicted in 2.9, the torques needed to compensate for the moment due to arm weight are:

$$\begin{cases} \tau_e = (\frac{W_{fore}}{2} + W_{hand})L_{fore} \cos(\varphi_1 + \varphi_2) \\ \tau_s = (\frac{W_{upper}}{2} + W_{fore} + W_{hand})L_{upper} \cos(\varphi_1) + \tau_e \end{cases} \quad (2.16)$$

Moreover, knowing the torques, it is possible to represent them as force thanks to the *Jacobian matrix* (J), defined as:

$$J = \begin{bmatrix} -L_{upper} \sin(\varphi_1) - L_{fore} \sin(\varphi_1 + \varphi_2) & -L_{fore} \sin(\varphi_1 + \varphi_2) \\ L_{upper} \cos(\varphi_1) + L_{fore} \cos(\varphi_1 + \varphi_2) & L_{fore} \cos(\varphi_1 + \varphi_2) \end{bmatrix} \quad (2.17)$$

Now, the x and y components of F can be computed as:

$$\begin{bmatrix} F_x \\ F_y \end{bmatrix} = (J^T)^{-1} \times \begin{bmatrix} \tau_s \\ \tau_e \end{bmatrix} \quad (2.18)$$

2.10 shows the new representation of the torques needed to counterbalance the gravity; the corresponding force F (*green*) is given by the computed x and y components and is applied at the wrist. F is the force needed to compensate the moment generated by the arm weight, therefore it produces the equivalent effect as τ_s and τ_e together.

Now, thanks to the previous description it is possible to display all Forces needed to compensate the arm weight in a vector field (2.11); the aim is to find the parameters that can optimally match the torques needed in the overall space.

In order to achieve accurate gravity compensation we show progressively more complex MARIONET combinations:

- The first one is developed using two different device, one applied from shoulder joint to the elbow, while the other from elbow to wrist.

²Total Body Mass

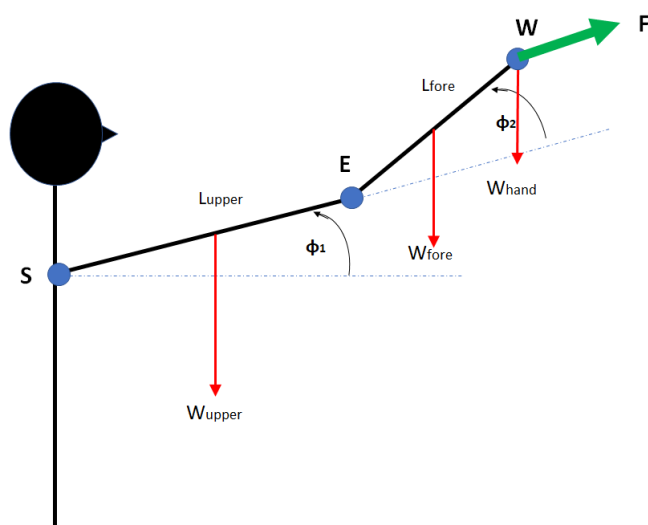


Figure 2.10: Free-body diagram that represents the torques as a force (F), as calculated through 2.18.

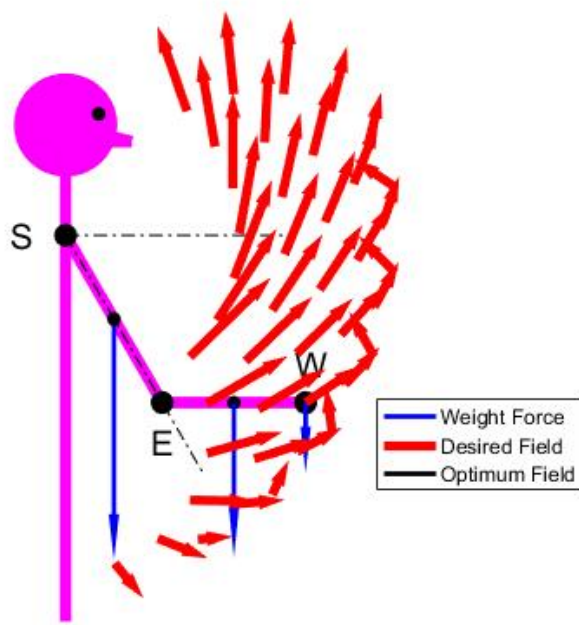


Figure 2.11: Vector field: each *red* arrow is the force at a certain shoulder–elbow angle couple able to compensate weight.

- The second is expected to require only one device, connecting the shoulder joint directly to wrist.

Both this solutions are based on the previously described algorithms (the two-parameter form), even if the calculation of the *Cost Function* changes with respect to the original form.

One-joint solution

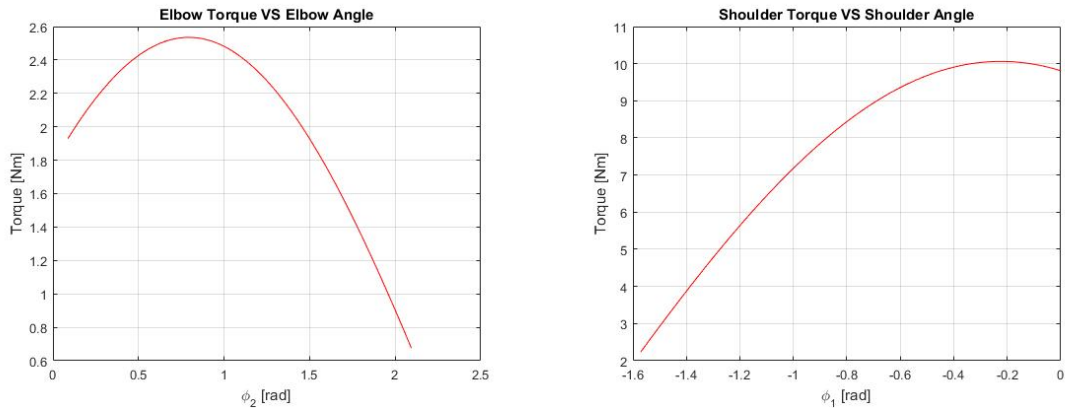
The first method final objective is to find two different sets of parameters (*Radius* R and *Angle* ϑ), one for each device, that, when given to the developed model, would be able to approximate the desired torques across the workspace; in order to do so, the calculation of the *cost function* had to undergo some changes. In fact, there was not just one profile to be estimated, but a series of different torques to be evaluated across the workspace, each of them corresponding to a point in the φ_1 - φ_2 space (shoulder and elbow angles). Therefore, the cost could not be calculated as the mere least squared errors between the device torque and one target torque, but it must be computed as the sum of the least squared errors throughout the space, for both the shoulder and elbow:

$$TotalCost_{elbow} = \sum_{i=1}^{N_{angles}} \sum_1^n (\tau_{tot} - DesiredTorque_i)^2, \quad (2.19)$$

$$TotalCost_{shoulder} = \sum_{i=1}^{N_{angles}} \sum_1^n (\tau_{tot} - DesiredTorque_i)^2, \quad (2.20)$$

Where N_{angles} is the number of elements in which the φ_1 and φ_2 ranges are divided. In this way it is possible to find the two optimal sets of parameters so as to have the best match in all the comprehensive gravity field. The target torques for the elbow joint are calculated by fixing one shoulder angle (φ_1) at a time, while varying the elbow one (φ_2) as presented in Figure 2.12a; on the other hand, the desired shoulder torques are obtained by fixing the elbow angle and altering the shoulder one (Figure 2.12b).

Eventually, the torques at the shoulder and at the elbow will be converted in forces



(a) Elbow torque profile obtained with a fixed shoulder angle $\varphi_1 = -0.7933rad$ (b) Shoulder torque profile obtained with a fixed elbow angle $\varphi_2 = 1.0807rad$

Figure 2.12: Elbow and Shoulder torque needed in order to compensate for gravity for fixed φ_1 and φ_2 respectively.

using 2.18 and will be scaled depending on the maximum force in the space (taking

into account desired and optimal forces at the same time) according to 2.21:

$$ScaledForce = \frac{Force}{MaxForce} \times 0.15, \quad (2.21)$$

where 0.15 is a scaling factor chosen to have a representation easy to understand. Since for certain $\varphi_1 - \varphi_2$ combinations the *JacobianMatrix* happens to be singular, the *MaxForce* can become infinite, hence making it impossible to have a good representation of the vector field; therefore, the points in which the matrix becomes singular are not taken into account.

Two-joint solution

The second solution, as previously explained, aims at approximating the torques able to compensate for the gravity using only one device connecting the shoulder with the wrist; the targets are the same ones shown in 2.12 for the elbow joint, while the one for the shoulder, in this case, is computed fixing the shoulder angle and varying the elbow one, as 2.13 shows.

In order to compute the set of optimal parameters, the cost function is calculated in

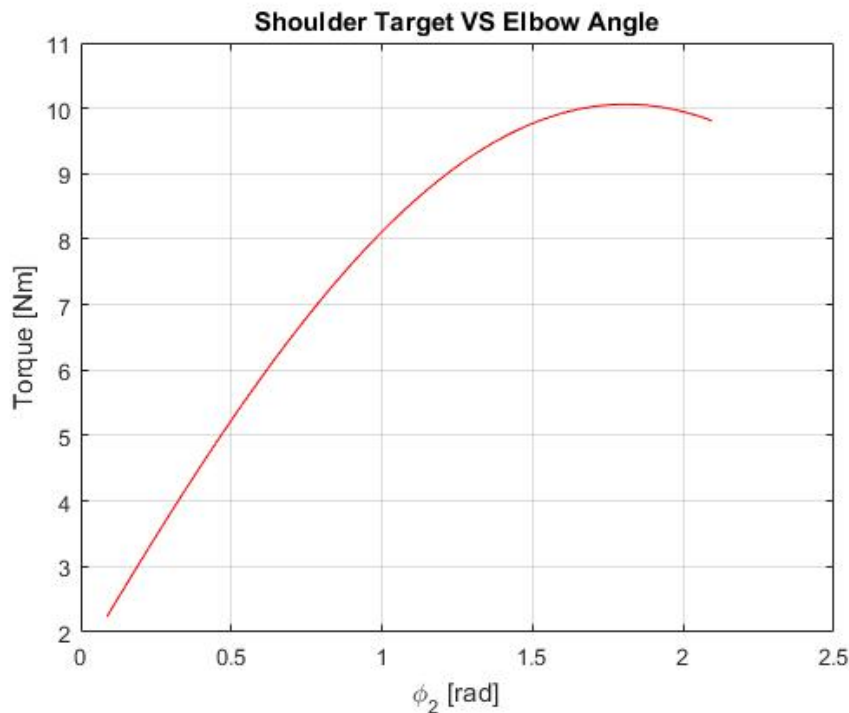


Figure 2.13: Target torque at the shoulder for the two-joints version.

the same way as before but for the fact that both the least squared errors evaluated on τ_s and τ_e are taken into account at the same time, therefore summing them in a unique total cost. So, the optimization algorithm has to minimize at the same time the costs

from the shoulder and elbow joints:

$$TotalCost_{elbow} = \sum_{i=1}^{N_{angles}} \sum_1^n (\tau_{tot} - DesiredTorque_i)^2, \quad (2.22)$$

$$TotalCost_{shoulder} = \sum_{i=1}^{N_{angles}} \sum_1^n (\tau_{tot} - DesiredTorque_i)^2, \quad (2.23)$$

$$TotalCost_{overall} = TotalCost_{shoulder} + TotalCost_{elbow}. \quad (2.24)$$

Complete device

Finally, the previously described devices are mixed so as to obtain the complete mechanism; the devices connect elbow and wrist, shoulder and elbow and shoulder and wrist. For the calculation of the cost function, all the previously explained methods are taken into account.

2.6 Experimental setup

2.6.1 Protocol

Through all the simulations the following quantities are taken: the stiffness of the spring, when not treated as a parameter is taken as $k = 500 \frac{N}{m}$, the length of the fore arm $L_{fore} = 0.26m$ and of the upper arm $L_{upper} = 0.36m$, the length of the spring in resting conditions $L_0 = 0.1m$ and the number of stacked elements $N = 5$.

2.6.2 Data analysis

In order to evaluate the performances of the simulations the *average absolute error* and the R^2 value were calculated.

The *average absolute error* should be as low as possible for the simulation to give good results. Moreover, the R^2 should be as close as possible to 1; this means that the trend of the solution matches the trend of the target.

Chapter 3

Results and Discussion

First, the results of the optimization algorithm are shown, both with two and three *parameters* for each stacked element. Then, the conclusions on the gravity compensation process are illustrated.

3.1 Optimization results

In this section, the results of the two (R and ϑ) and three (R , ϑ and *stiffness* k) parameters problems are presented, focusing in addition on some solutions connected to the problems of local minima; eventually a discussion on the optimal number of stacked elements is delineated.

3.1.1 Simulation with two Parameters: *Radius* and *Angle* ϑ

The first case is meant to demonstrate the process in the simplest manner; an elbow device is taken into account and the chosen parameters are R and ϑ ; other quantities that is important to point out, set manually by the user, are the stiffness $k = 500 \frac{N}{m}$, the length of the fore arm $L_{fore} = 0.26m$, the length of the spring in resting conditions $L_0 = 0.1m$ and the number of stacked elements $N = 5$ (resulting in a total of $M = 10$ parameters to be found).

By stacking 5 different MARIONETs (3.1, in *blue*) it is possible to approximate the target (*red*). The error, defined as the difference between the target and the exerted torque, is pictured.

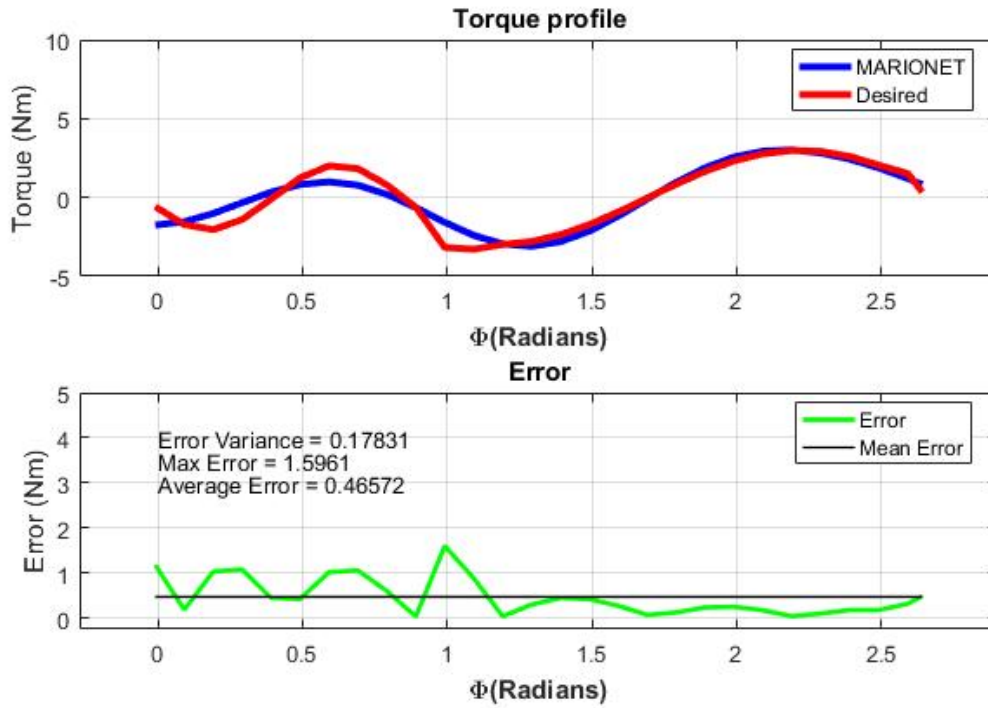


Figure 3.1: Top: in *blue* the torque generated by 5 MARIONETs, in *red* the target one. Bottom: the error (in *green*), calculated as the difference between the red and blue profiles, and the average error (*black* line); moreover, some information about the error are shown.

The *blue* shape is obtained with the parameters listed in 3.1, in 3.2 the arrangement of the MARIONETs is pictured and in 3.3 each single component is shown.

Table 3.1: OPTIMAL PARAMETERS FOR EACH SINGLE COMPONENT.

	$R[m]$	$\vartheta[rad]$
MARIONET1	0.1000	0.9407
MARIONET2	0.1000	3.2715
MARIONET3	0.1000	-1.5443
MARIONET4	0.1000	-0.3755
MARIONET5	0.0878	2.2786

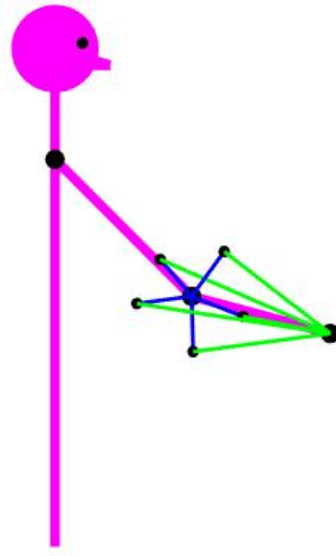


Figure 3.2: How the MARIONETs are arranged in the space: in *blue* is the parameter R and in *green* is the spring.

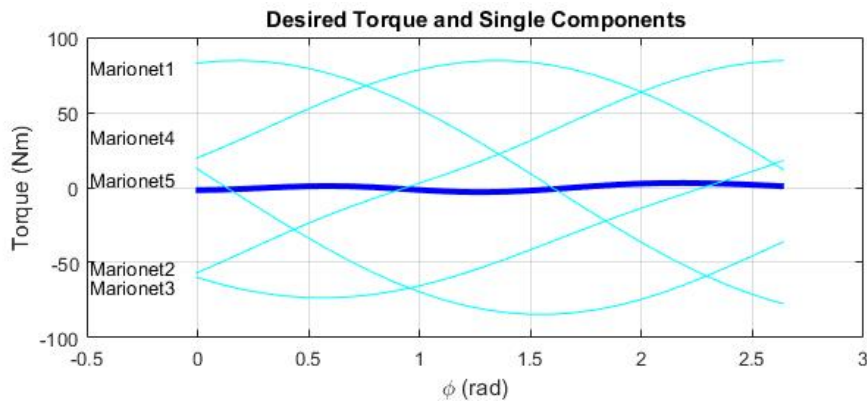


Figure 3.3: Top: in *blue* the overall torque generated by 5 MARIONETs is represented, while in *cyan* each single component is pictured.

An average error of $0.4657Nm$ was obtained, with a variance $\sigma^2 = 0.17831N^2m$. Furthermore, it presents an average percentage error of 54%, which may seem high, but it is probably due to the fact that the desired torque profile had sharp changes, which is difficult to replicate with sinusoidal-like functions. In order to prove this thesis, a smoother target torque profile was used; in this case, the algorithm was able to achieve an average error of $0.0717Nm$ with a variance $\sigma^2 = 0.0028$ and the average percentage error is only 1.3087%. In fact, from 3.4 it is possible to see that the two torques were almost completely overlapped, while the error was nearly null everywhere.

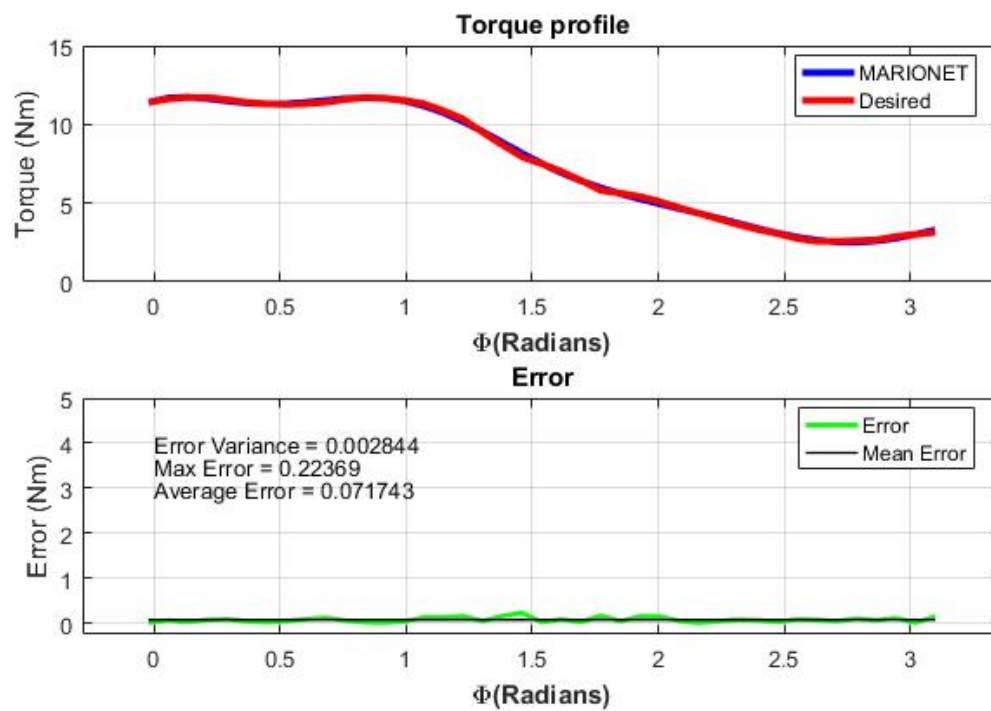


Figure 3.4: Results obtained with a smoother target torque. *Top:* the two torque fields were almost completely overlapped. *Bottom:* A smoother target resulted in smaller errors.

3.1.2 Simulation with three Parameters: *Radius*, *Angle* ϑ and *Stiffness* k

Considerations made in sections 3.1.1 and 3.1.3 were still valid when adding a third parameter for each stacked MARIONET, which is the stiffness k of the each spring. Having more variables to work on, this adaptation of the algorithm was better. Average error was slightly lower than the one in 3.1 (3.5 shows the results), with a value of $0.42417Nm$ (corresponding to a 43.6986% percentage error). In 3.2, the obtained parameters are reported.

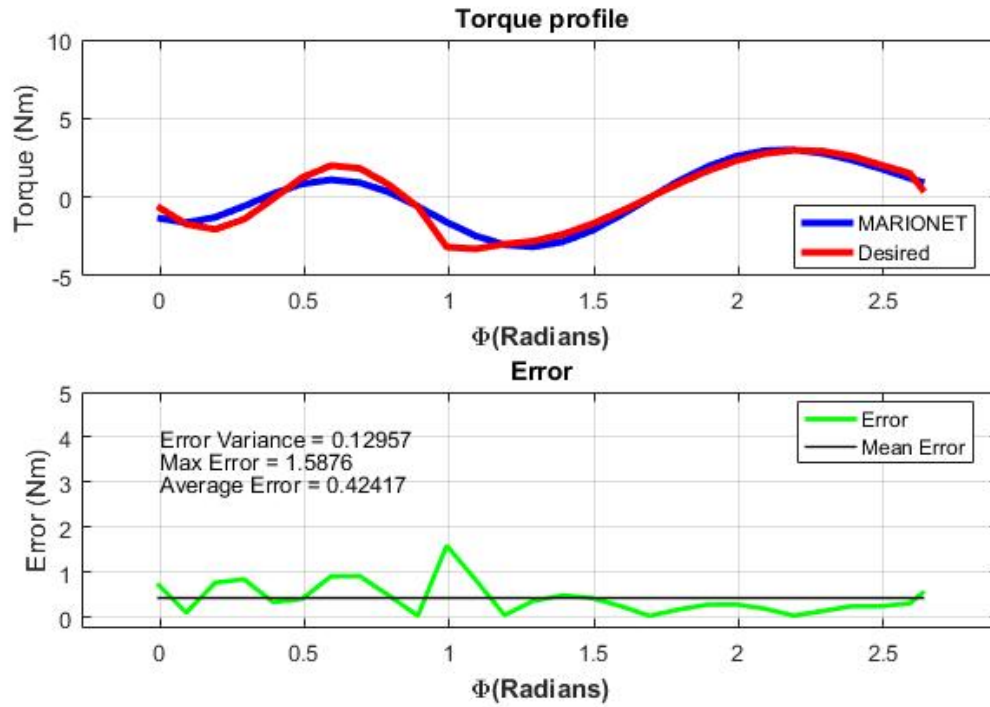


Figure 3.5: Top: in *blue* the torque generated by 5 MARIONETs, each tuned according to three parameters R , ϑ and k , in *red* the target one. Bottom: the error (in *green*), calculated as the difference between the red and blue profiles, and the average error (*black* line); moreover, some information about the error is shown.

Table 3.2: OPTIMAL PARAMETERS FOR EACH SINGLE COMPONENT.

	$R[m]$	$\vartheta[rad]$	$k[\frac{N}{m}]$
MARIONET1	0.10	-5.3266	533
MARIONET2	0.10	-0.5275	1000
MARIONET3	0.10	2.9027	50
MARIONET4	0.07	3.8921	1000
MARIONET5	0.09	3.7753	1000

The drawback of this version of the algorithm, obviously, is that the computational weight and time to process increased. Considering that the error calculated through this

method did not decrease so dramatically and that the achieved results are almost the same, it seems unproductive to spend more resources using this version of the algorithm instead of the original.

3.1.3 How many stacked MARIONETs?

As more and more MARIONETs were stacked, the smaller the error got. We tested it (3.6); average error decreased less as the number of stacked elements increased. The error passed from $1.7721Nm$ with only one MARIONET to $0.3169Nm$ with ten. After five or six stacked elements the results approached a *plateau* and the decrease in error became small. These results were obtained solving the optimization problem with two parameters for each stacked element, with the same data and target profile reported in section 3.1.1.

In 3.3 all the errors are reported.

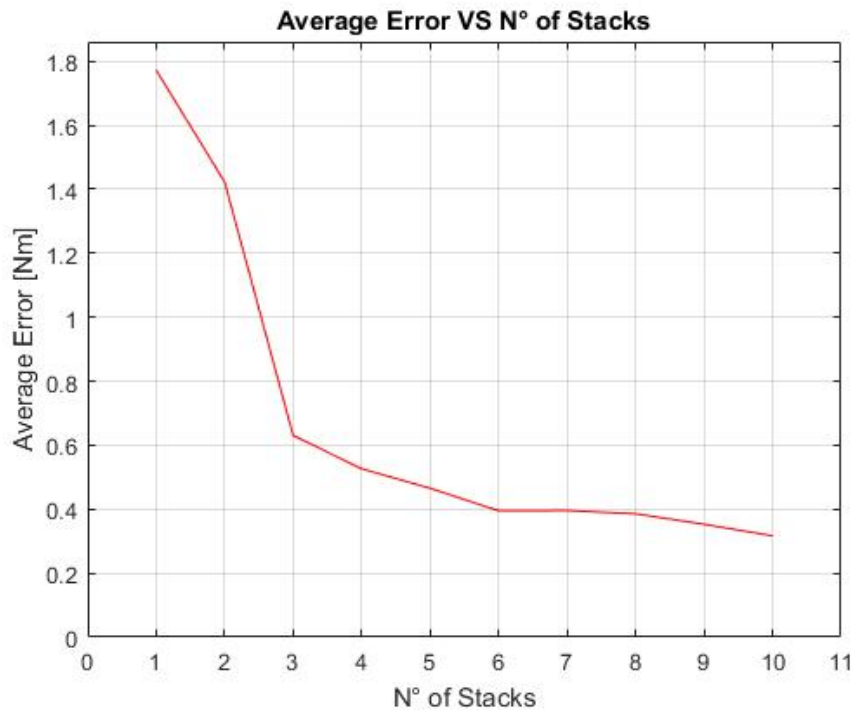


Figure 3.6: Trend of the average error with respect to the the number of stacked elements: each point represents the average absolute error as obtained with a certain number of stacked elements.

Table 3.3: AVERAGE ERROR [Nm] WITH RESPECT TO THE NUMBER OF STACKED ELEMENTS.

Stacked MARIONETs	Average Error [Nm]	Stacked MARIONETs	Average Error [Nm]
1	1.7721	6	0.3951
2	1.4225	7	0.3958
3	0.6304	8	0.3855
4	0.5263	9	0.3528
5	0.4653	10	0.3169

Since patients need to feel comfortable wearing the device, the number of MARIONETs composing the mechanism can not be too high. Moreover, a high number of components

would result in an increased computational cost and time. This trade-off between error and complexity seems to be the point where the *plateau* starts, so choosing a five element solution appears to be optimal.

3.1.4 Problems connected to random initialization

Since the optimization algorithm starts with a random guess for the initial parameters, some concerns are to be addressed. In fact, the results of the process highly depend on the starting point.

A way to overcome this problem was developed: 3.7 shows the method adopted. The optimization algorithm previously developed was inserted into a "for" loop whose number of iteration N_{iter} has to be decided by the user; at each iteration i , a set of optimal parameters is found, the average error is calculated and compared to the minimum mean error previously found. Eventually, when $i > N_{iter}$, the set of parameters corresponding to the minimum average error is taken.

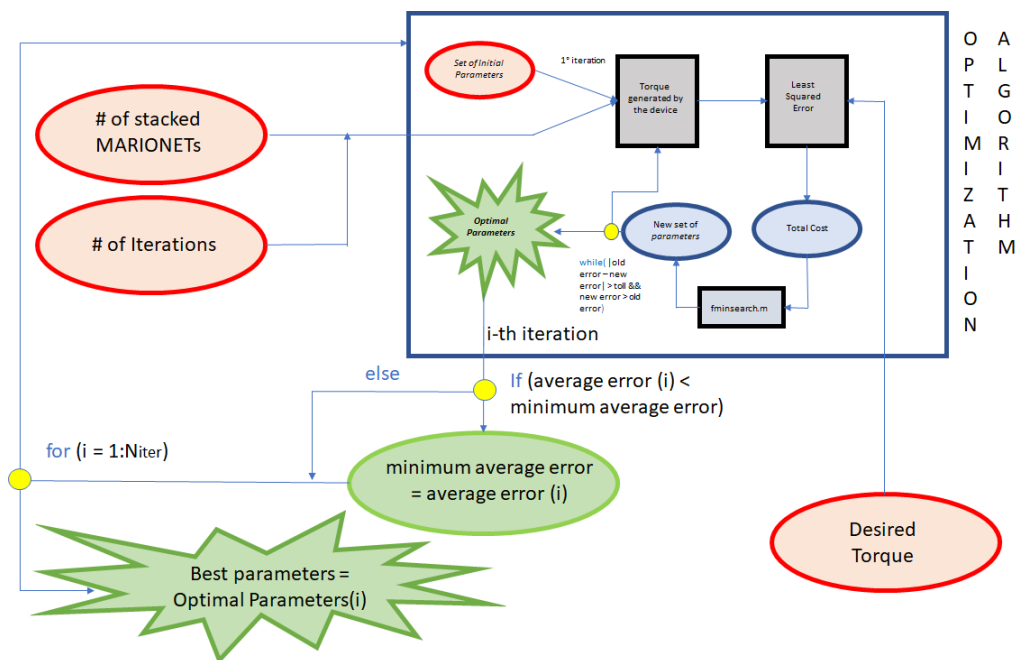


Figure 3.7: Flow chart of the developed algorithm.

To prove the fact that the results highly depend on the set of initial parameters, the average error for each i^{th} iteration is calculated and plotted, with $N_{iter} = 200$. Therefore, the trend of the error is shown and the maximum (*blue* circle) and the minimum (*green* circle) are highlighted; as the image points out, the error varies dramatically between different iterations with a variance $\sigma^2 = 0.0197$.

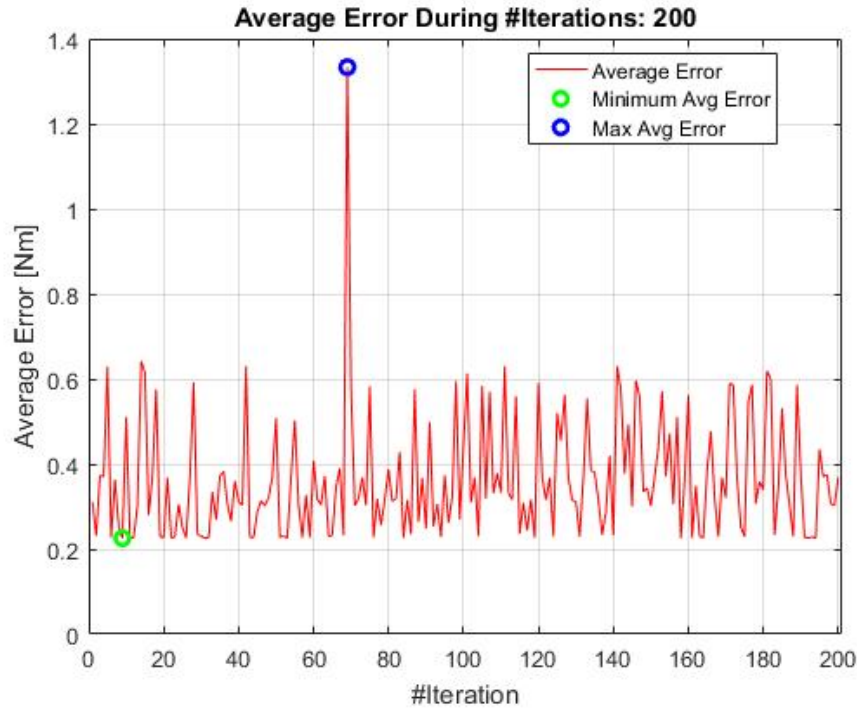
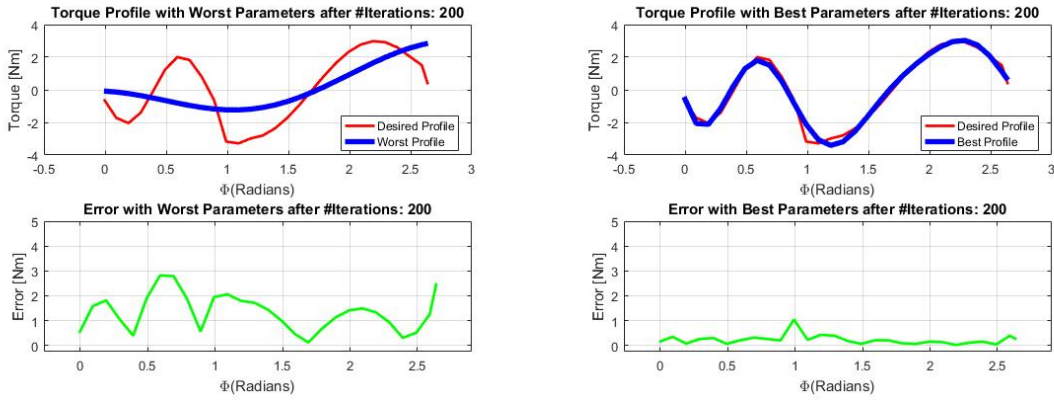


Figure 3.8: Average error for each iteration.

3.9 pictures what we previously noted: 3.9a displays the torque and error obtained with a set of parameters which is clearly non-optimal (*blue* circle of 3.8), while 3.9b shows a successful run of the algorithm with a optimal set of parameters (*green* circle of 3.8).

These results demonstrate the need for multiple iterations of the optimization algorithm and, moreover, it suggests that one can successfully find a globally optimal solution to the problem.



(a) Torque and error obtained with non-optimal parameters (b) Torque and error obtained with optimal parameters

Figure 3.9: Comparison of the result of two different output of the algorithm.

3.2 Gravity compensation results

Here the results of the gravity compensation are presented, taking into account three different configurations for the device. At first, a disposition of two one-joint is studied, followed by a two-joints device; finally, a mixed mechanism presenting both the previous configurations is taken into account

3.2.1 One-joint solution

The algorithm was run with the same specifications presented in section 3.1.1 for the elbow device, while the length of upper arm $L_{upper} = 0.35m$ was used for the shoulder device; in addition, a $TBM = 70Kg$ was chosen, so as to find the weight of the different parts of the arm using 2.13–2.12. Moreover, in order to represent the vector field, the range of φ_1 ($[-\frac{\pi}{2}; 0]$) and the one of φ_2 ($[0; \frac{2\pi}{3}]$) were divided in 7 points, so as to have a total of 49 points in which the torques could be evaluated.

Running the algorithm, the two set of parameters were found. Moreover the absolute average error both in $[Nm]$ and $[\%]$ and the coefficient of determination R^2 are calculated; R^2 is computed as:

$$R^2 = 1 - \frac{SS_{res}}{SS_{tot}} \quad (3.1)$$

being SS_{tot} is the sum of squared total and SS_{res} is the sum of squared residuals. This coefficient expresses the amount of variance explained by the model and it will be used in the next paragraphs as the discriminating factor to find the best and the worst approximations.

Elbow Device

In 3.4 the average error, both in Nm and percentage, and the coefficient of determination are shown for the elbow joint, with the first column representing the fixed shoulder angles at which each torque profile is calculated. Some percentage errors are not reported because to be calculated they had to be divided by zero (3.2); in fact, being the target torque zero in some point and being

$$Err(\%) = \left| \frac{TargetTorque - OptimalTorque}{TargetTorque} \right| \times 100, \quad (3.2)$$

the resulting error would be $\approx \infty$, making it useless for any possible evaluation.

Table 3.4: AVERAGE ERROR [Nm], AVERAGE ERROR [%] AND R^2 FOR EACH PROFILE FOR ELBOW TORQUE.

Shoulder Angle [rad]	Avg Abs. Error [Nm]	Avg Abs Error [%]	Coeff. of Determination
-1.5708	0.9819	—	-0.6198
-1.3090	0.6947	47.8814	-0.6330
-1.0472	0.4136	23.4124	0.0447
-0.7854	0.2493	13.1673	0.8178
-0.5236	0.3793	—	0.7629
-0.2618	0.6941	115.2472	0.5224
0	1.0543	139.5801	0.2127

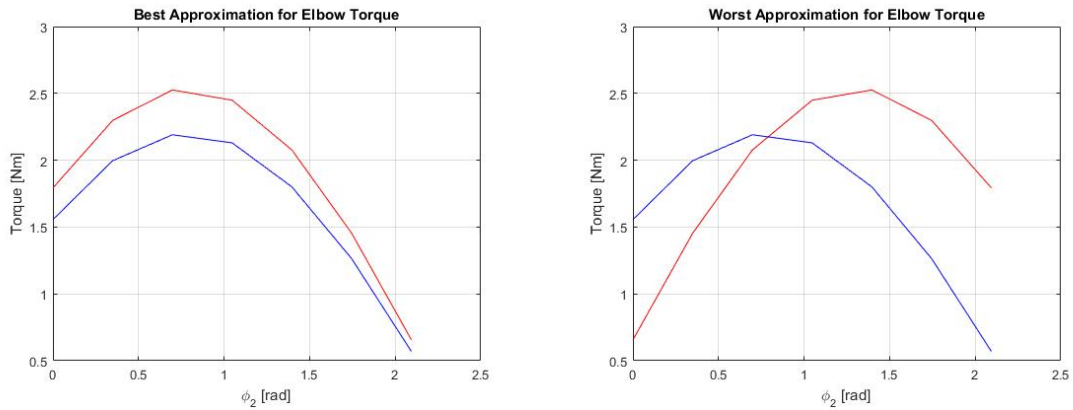
Moreover, in 3.5 the optimal parameters for the elbow device are reported.

Table 3.5: OPTIMAL PARAMETERS FOR GRAVITY COMPENSATION AT THE ELBOW JOINT.

	$R[m]$	$\vartheta[rad]$
MARIONET1	0.0707	-0.2002
MARIONET2	0.0713	-2.1304
MARIONET3	0.0517	-4.2258
MARIONET4	0.0598	0.8025
MARIONET5	0.05	-1.3452

As it can be noted, the error varies greatly throughout the overall space, from a minimum of $0.2493Nm$ ($\approx 13\%$) to a maximum of $1.0543Nm$ ($\approx 139\%$); this happens, probably, because the algorithm tries to approximate one of the profiles more than another leading to a great diversity in the performances. This can be simply perceived thanks to 3.10 where the best and worst match are shown. In fact, in Figure 3.10a it can be seen that the two profiles are very similar both in the trend and in the magnitude

(showing a $R^2 = 0.8178$), whereas in Figure 3.10b the two differs greatly in every aspect ($R^2 = -0.6198$); in fact, the calculated coefficient is negative, meaning that the resulting model behaves worst than how the mean would.



(a) Elbow torque corresponding to the best approximation.

(b) Elbow torque corresponding to the worst approximation.

Figure 3.10: Elbow torques that are approximated in the best and worst way, respectively.

Shoulder Device

The process was repeated for the shoulder device; in 3.6 the average errors are detailed for the shoulder joint. All the considerations previously made for the elbow device are still valid now for the shoulder equipment; the error, anyway, seems to be smaller with respect to the previous situation, with a minimum error of $0.4231Nm$ ($\approx 9\%$) and a maximum of $1.2167Nm$ (19,424%) (unfortunately not presenting a percentage error for the aforementioned problem).

Table 3.6: AVERAGE ERROR [Nm] AND AVERAGE ERROR [%] FOR EACH PROFILE FOR SHOULDER TORQUE.

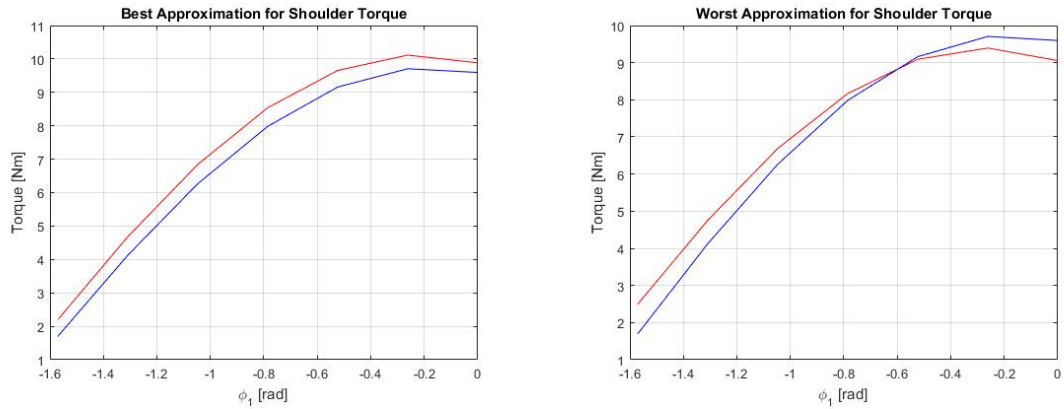
Elbow Angle [rad]	Avg Abs. Error [Nm]	Avg Abs Error [%]	Coeff. of Determination
0	0.9774	—	0.9188
0.3491	0.7186	20.5659	0.9450
0.6981	0.5683	6.8169	0.9580
1.0472	0.4826	8.7986	0.9691
1.3963	0.4231	9.1378	0.9599
1.7453	0.7246	12.5672	0.8388
2.0944	1.2167	19.424	0.4413

Furthermore, as in the elbow device case, the parameters for the shoulder device are shown in 3.7.

Table 3.7: OPTIMAL PARAMETERS FOR GRAVITY COMPENSATION AT THE SHOULDER JOINT.

	$R[m]$	$\vartheta[rad]$
MARIONET1	0.05	-0.4645
MARIONET2	0.0843	4.2597
MARIONET3	0.0957	2.7545
MARIONET4	0.0723	4.9682
MARIONET5	0.5	-0.0478

The same consideration that were done in the case of the elbow device are still valid for the shoulder system; in 3.11 the best ($R^2 = 0.9691$) and the worst ($R^2 = 0.4413$) approximation respectively are shown. What can be noted is that the obtained results seems to be quite satisfying for both the best and the worst case.



(a) Shoulder torque corresponding to the best approximation.

(b) Shoulder torque corresponding to the worst approximation.

Figure 3.11: Shoulder torques that are approximated in the best and worst way, respectively.

Once the shoulder and elbow torque were obtained, they were converted into force using 2.18, so as to picture a vector field as explained in section 2.5 and shown in 3.12. The picture shows the vector field needed to compensate for gravity (in *red*) and the one obtained through the optimization algorithm (in *black*); it can be noted that the optimization seems to work better and better as the shoulder angle increases. Furthermore, the obtained torques do not results in a satisfying approximation especially for the most extreme points (for example, those where the arm is completely stretched).

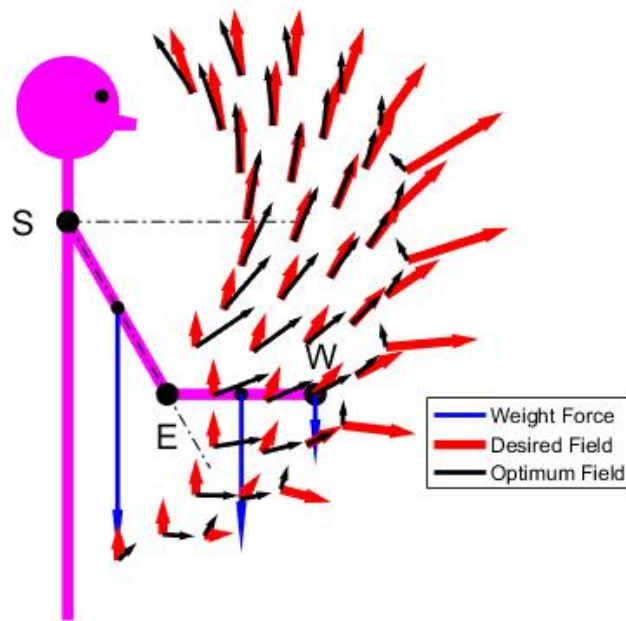


Figure 3.12: Vector field that we want to achieve (in *red*) and optimal field obtained with the algorithm (in *black*).

3.2.2 A MARIONET crossing two joints

The solution implementing the two-joints method is, then, applied to the gravity compensation problem; the specifications are the same as in section 3.1.1 except for the resting length of the spring that was set to be $L_0 = 0.4m$, longer than the previous case, since it has to link two points that are more distant than before. 3.13 shows the arrangement of the two-joint device compared to the one-joint version.

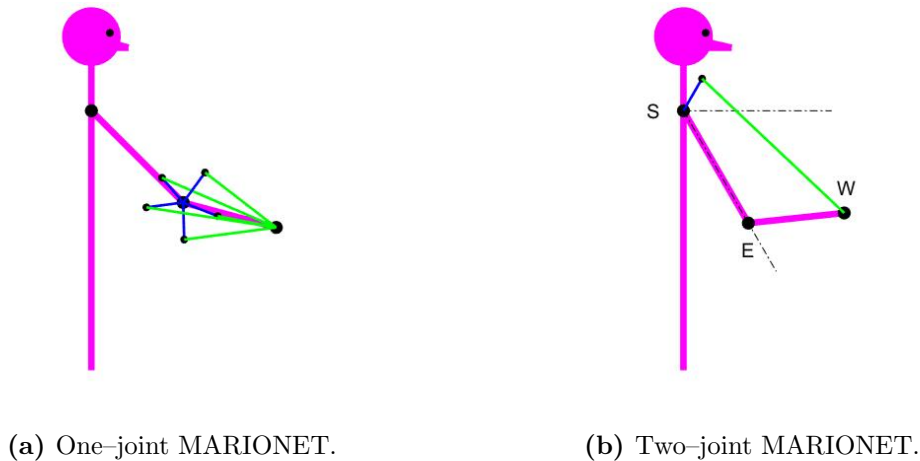
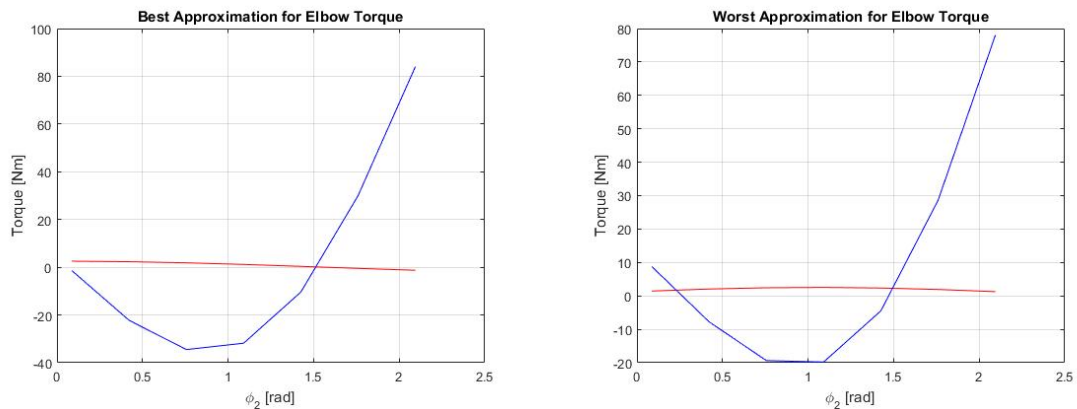


Figure 3.13: Arrangement of a one-joint and two-joint MARIONETs.

Since only one optimal set of parameters had to be found taking into account both shoulder and elbow torque in the overall space, the results of a two-joint MARIONET by itself were expected to be highly non-satisfying.

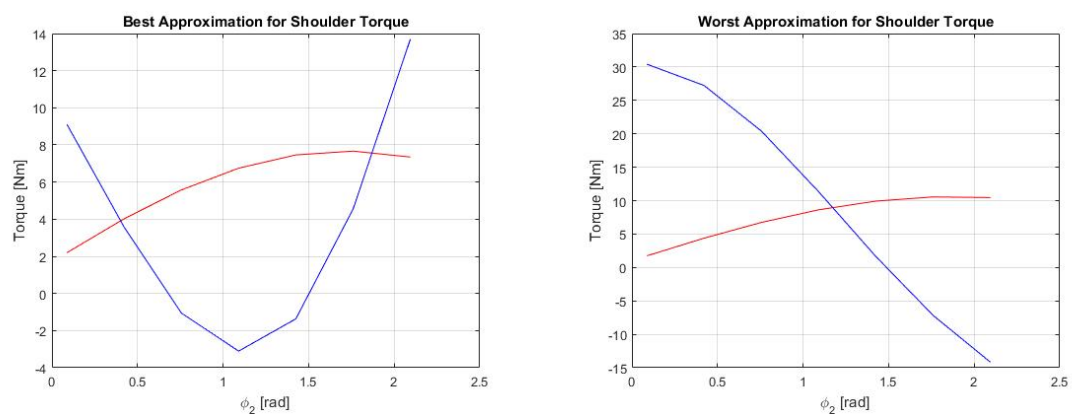
As predicted, the obtained set of parameters was unable to suitably approximate the desired field needed to compensate for the weight of the arm. This was particularly true in the case of the torque at the elbow, as 3.16 shows; in fact it can be seen that even where the error was at its minimum ($22.4681Nm$) the MARIONET was not able to approximate nor the magnitude of the desired torque nor its trend (Figure 3.16a), as pointed out by the R^2 which is highly negative in this case. In Figure 3.16b the worst situation is pictured, showing an average error of $32.0597Nm$.

Furthermore, the approximation of the shoulder torque (depicted in 3.16) is still unsatisfying; in the best case, in fact, the average error is $6.0210Nm$ (Figure 3.16c), while in the worst one it reaches $20.0612Nm$ (Figure 3.16d), with an $R^2 = -11.3297$ in the best case, which means that the model is completely not suited to approximate the desired torque field.



(a) Elbow torque corresponding to the best approximation for the two-joint case.

(b) Elbow torque corresponding to the worst approximation for the two-joint case



(c) Shoulder torque corresponding to the best approximation for the two-joint case.

(d) Shoulder torque corresponding to the worst approximation for the two-joint case

Figure 3.14: Attempts to cancel gravity: the large amount of error suggests that a two-joint MARIONET by itself cannot provide adequate gravity cancellation (color convention match previous figures).

Finally, 3.17 shows the desired vector field (*red*) and the one obtained through the algorithm implementing the two-joints solution; as previously noted, the overall resolution is clearly non-optimal and the picture strengthen the certainty.

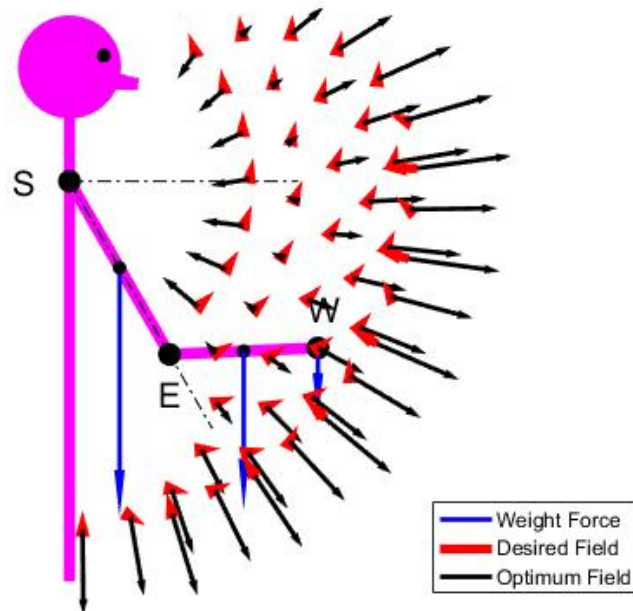
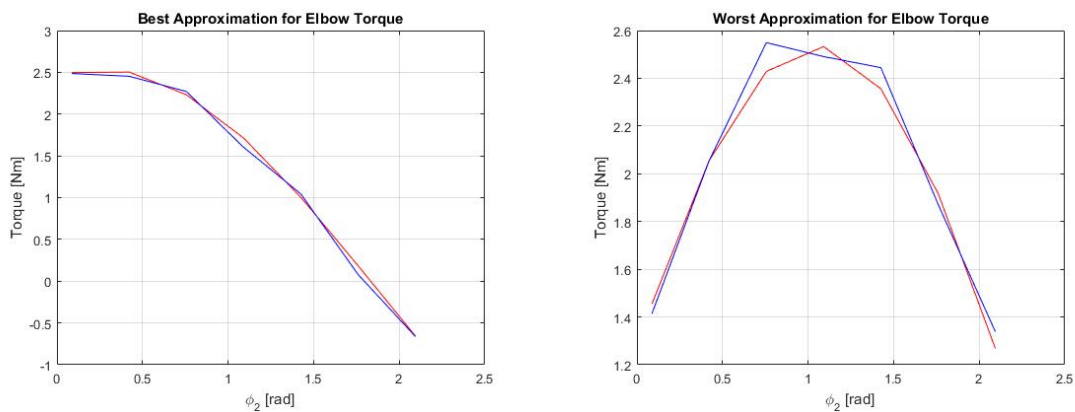


Figure 3.15: Vector field that we want to achieve (in *red*) and optimal field (in *black*) as obtained through the two-joints version of the algorithm; adequate gravity cancellation appears to be difficult with this mechanism by itself.

3.2.3 A complete MARIONET

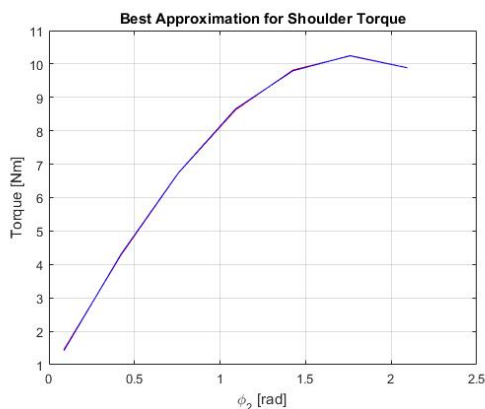
The final solution for the gravity compensation problem, which comprehends the aforementioned complete device, is finally applied. The final mechanism puts together the previous configuration — shoulder–elbow, elbow–wrist (one–joint) and shoulder–wrist (two–joints) — in order to achieve a result that can totally compensate the weight of the patient’s arm. For this part of the study, 5 MARIONETs are taken into account in each configuration and the same setting as before are used. Under these conditions, it is possible to verify that the model is highly satisfying; in fact, the obtained parameters are able to approximate the desired field needed.

Starting from the elbow, it is possible to evaluate that the model as high performances; in fact, the $R^2 = 0.9968$ and the absolute average error of $0.0516Nm$, found for the best possible approximation, indicate that the proposed device is able to estimate the torque needed for the gravity compensation. Moreover, even for the worst case, the obtained value $R^2 = 0.9771$ demonstrates that the model is able to achieve gravity compensation.

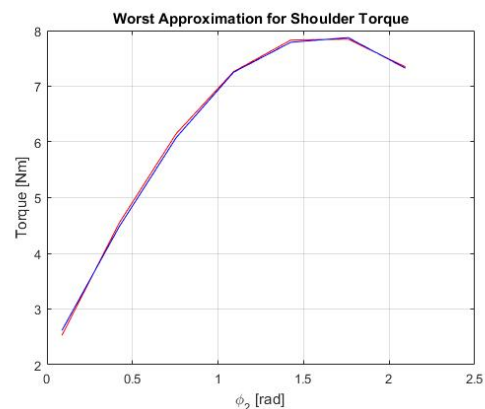


(a) Elbow torque corresponding to the best approximation for the two–joint case.

(b) Elbow torque corresponding to the worst approximation for the two–joint case



(c) Shoulder torque corresponding to the best approximation for the two–joint case.



(d) Shoulder torque corresponding to the worst approximation for the two–joint case

Figure 3.16: Final attempt to cancel gravity: the mixed device seems able to compensate for arm weight (color convention match previous figures).

Finally, taking a look to the obtained vector field, it is possible to note that the proposed solution is the best between the ones shown. In fact, the (*red*) arrows and the (*black*) ones perfectly overlap.; this means that it is possible to achieve gravity compensation mixing the previous mechanisms.

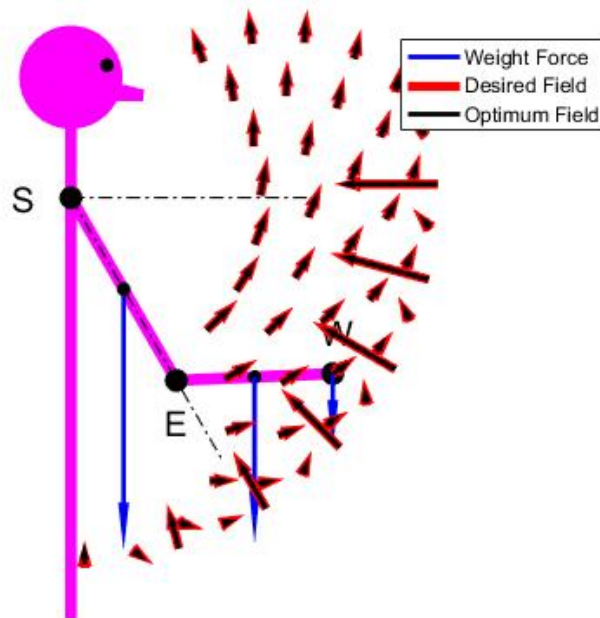


Figure 3.17: Vector field that we want to achieve (in *red*) and optimal field (in *black*) as obtained through the mixed version of the algorithm; adequate gravity is achievable with this mechanism.

Chapter 4

Conclusions and future development

Nowadays, more and more people are in need for rehabilitation, a necessary tool for restoration of the functional capacity. In order to meet this compelling need, robotic devices are employed not only to facilitate and accelerate rehabilitation, but also to achieve better results where previous therapies failed.

The MARIONET is a simple mechanism able to exert customized torque profiles to the patient's limbs by adjusting the moment arm in order to obtain torque. Here, the MARIONET is expanded so as to obtain a portable system, completely passive and customizable to the needs and disabilities of the patient. Not only this device is thought to fit into a large variety of anthropometric dimensions, but also to achieve different tasks, such as assistance, error augmentation and gravity compensation.

Since a MARIONET is able to exert a sinusoidal torque field, the possibility of "stacking" a certain number of devices is taken into account so as to obtain more complex torques; this concept is similar to a truncated Fourier Transform, with each mechanism acting as a basis function.

The ability to achieve complicated torque profiles and the possibility to tune each single element according to certain specifications led to development of an optimization algorithm able to compute a set of optimal parameters which, in turn, could be used to customize the device on the patient's need.

This algorithm was proven to be able to obtain interesting outcomes resulting in the approximation of the different target profiles with which it was fed. The method was not only tested on "hand-made" torque profiles, but also on the moments generated by a person's muscles and whose aim is to compensate the weight of the human arm.

Different versions of the algorithm, corresponding to as many adaptations of the device, were developed and were able to evaluate one-joint or two-joints mechanism or to compute two or three parameters for each stacked elements. The one-joint version with two parameters resulted the best solution to approximate torque fields, presenting

the lower computational work and the smaller time to process, despite a slightly worst error with respect of the three parameters version. Furthermore, for what concerns the number of stacked MARIONETs the trade-off between the error and the comfort of the user resulted in five or six elements composing the total device.

Finally, the two-joints version alone resulted to be not suited to achieve gravity compensation, while with the two single joint devices the approximation seems more satisfying. Anyway, the best possible solution could be obtained by the model which included both the previous designs of the MARIONET.

The works that remains to do will be focused on the actual design and physical realization of the MARIONET device (4.1) and a clinical trial able to assess the real possibilities of the described mechanism; right know, the device is being developed at the Shirley Ryan Ability Lab in Chicago (former Rehabilitation institute of Chicago) by the team of the Robotics Lab guided by Professor James L. Patton. Fig. 4.2 shows the first prototype of the mechanism in a configuration such that it is able to compensate for the weight of the arm of the manikin.

More work will be done on the optimization algorithm to make it more efficient , leading to the opportunity of using the more complex versions. Furthermore, since the resting length and stiffness of the springs seems to have a strong impact on the final approximations, a version of the algorithm should be designed so as to implement those specifications as parameters.

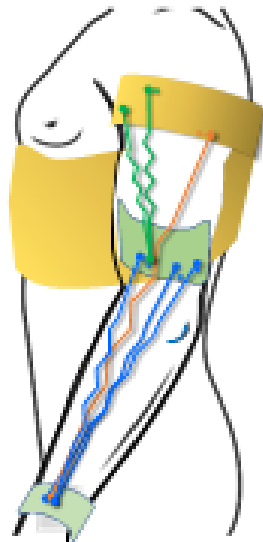


Figure 4.1: A possible design of the MARIONET.

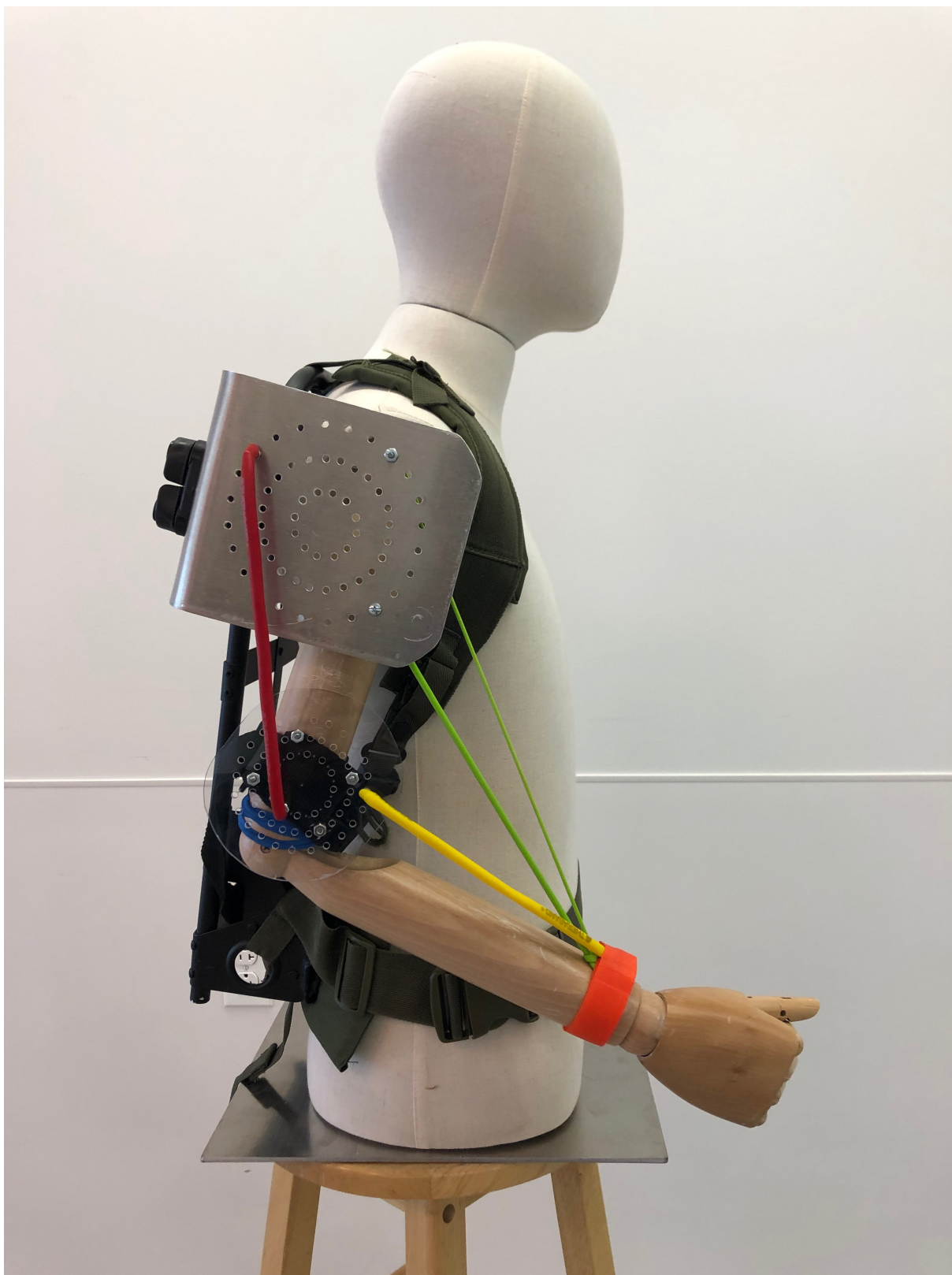


Figure 4.2: The first prototype of the MARIONET is being developed at the Shirley Ryan Ability Lab; in this picture it is possible to see the complete device with the mixed configurations.

Acronimi

ADLs	Activities of Daily Living
MARIONET	Moment arm Adjustment for Remote Induction Of Net Effective Torque
MIME	Mirror-Image Motion Enabler
DoF	Degrees of Freedom
SEA	Series Elastic Actuators
CoR	Center of Rotation
TBM	Total Body Mass
T-WREX	Therapy Wilmington Robotic Exoskeleton

Bibliography

- [1] D. et al. Mozaffarian. Heart disease and stroke statistics–2016 update. *Circulation*, 133:e38–e360, 2016.
- [2] V. L. et al. Roger. Heart disease and stroke statistics–2012 update. *Circulation*, 125:e2–e220, 2012.
- [3] Margaret Kelly-Hayes, Alexa Beiser, Carlos S Kase, Amy Scaramucci, Ralph B D’Agostino, and Philip A Wolf. The influence of gender and age on disability following ischemic stroke: the framingham study. *Journal of Stroke and Cerebrovascular Diseases*, 12(3):119 – 126, 2003.
- [4] D. Foti, L. W. Pedretti, and S. M. Lillie. Activities of daily living. *Occupational therapy: Practice skills for physical dysfunction*, pages 463–506, 1996.
- [5] Amanda G Thrift, Tharshanah Thayabaranathan, George Howard, Virginia J Howard, Peter M Rothwell, Valery Feigin, Bo Norrving, Geoffrey Donnan, and Dominique Cadilhac. Global stroke statistics. 12, 10 2016.
- [6] Jonathan W Sturm, Geoffrey A Donnan, Helen M Dewey, Richard A L Macdonell, Amanda K Gilligan, Velandai Srikanth, and Amanda G Thrift. Quality of life after stroke: the north east melbourne stroke incidence study (nemesis). *Stroke*, 35(10):2340 – 2345, 2004.
- [7] T. K. Tatemichi., D. W. Desmond, Y. Stern, M. Paik, M. Sano, and E. Bagiella. Cognitive impairment after stroke: frequency, patterns, and relationship to functional abilities.
- [8] Cathy L. Bays. Quality of life of stroke survivors: a research synthesis. 2001.
- [9] H. Rigby, G. Gubitz, G. Eskes, Y. Reidy, C. Christian, V. Grover, and S. Phillips. Caring for stroke survivors: Baseline and 1-year determinants of caregiver burden. *International Journal of Stroke*, 4(3):152–158, 2009. PMID: 19659814.
- [10] M. Murie-Fernández, P. Irimia, E. Martínez-Vila, M. John Meyer, and R. Teasell. Neuro-rehabilitation after stroke. *Neurología (English Edition)*, 25(3):189 – 196, 2010.
- [11] B.T. Volpe, H.I. Krebs, N. Hogan, L. Edelstein, C. Diels, and M. Aisen. A novel approach to stroke rehabilitation. *Neurology*, 54(10):1938–1944, 2000.
- [12] Hermano Igo Krebs, Mindy L. Aisen, Bruce T. Volpe, and Neville Hogan. Quantization of continuous arm movements in humans with brain injury. *Proceedings of the National Academy of Sciences*, 96(8):4645–4649, 1999.

- [13] P. S. Lum, C. G. Burgar, M. Van der Loos, P. C. Shor, M. Majmundar, and R. Yap. The mime robotic system for upper-limb neuro-rehabilitation: results from a clinical trial in subacute stroke. In *9th International Conference on Rehabilitation Robotics, 2005. ICORR 2005.*, pages 511–514, June 2005.
- [14] Stefano Mazzoleni, Patrizio Sale, Marco Franceschini, Samuele Bigazzi, Maria Chiara Carrozza, Paolo Dario, and Federico Posteraro. Effects of proximal and distal robot-assisted upper limb rehabilitation on chronic stroke recovery. *33*, 06 2013.
- [15] T. George Hornby, Donielle D. Campbell, Jennifer H. Kahn, Tobey Demott, Jennifer L. Moore, and Heidi R. Roth. Enhanced gait-related improvements after therapist- versus robotic-assisted locomotor training in subjects with chronic stroke. *Stroke*, 39(6):1786–1792, 2008.
- [16] Laura Marchal-Crespo and David J. Reinkensmeyer. Review of control strategies for robotic movement training after neurologic injury. *Journal of NeuroEngineering and Rehabilitation*, 6(1):20, Jun 2009.
- [17] Susan Fasoli, Hermano I Krebs, Joel Stein, Walter Frontera, and Neville Hogan. Effects of robotic therapy on motor impairment and recovery in chronic stroke. *84*:477–82, 04 2003.
- [18] Jeremy L. Emken, Raul Benitez, and David J. Reinkensmeyer. Human-robot cooperative movement training: Learning a novel sensory motor transformation during walking with robotic assistance-as-needed. *Journal of NeuroEngineering and Rehabilitation*, 4(1):8, Mar 2007.
- [19] B. Vanderborght, A. Albu-Schaeffer, A. Bicchi, E. Burdet, D. G. Caldwell, R. Carloni, M. Catalano, O. Eiberger, W. Friedl, G. Ganesh, M. Garabini, M. Grebenstein, G. Grioli, S. Haddadin, H. Hoppner, A. Jafari, M. Laffranchi, D. Lefeber, F. Petit, S. Stramigioli, N. Tsagarakis, M. Van Damme, R. Van Ham, L. C. Visser, and S. Wolf. Variable impedance actuators: A review. *Robot. Auton. Syst.*, 61(12):1601–1614, December 2013.
- [20] Jae Hoon Lee, Christian Wahrmund, and Amir Jafari. A novel mechanically overdamped actuator with adjustable stiffness (mod-awas) for safe interaction and accurate positioning. *Actuators*, 6(3), 2017.
- [21] J. S. Sulzer, M. A. Peshkin, and J. L. Patton. Marionet: An exotendon-driven rotary series elastic actuator for exerting joint torque. In *9th International Conference on Rehabilitation Robotics, 2005. ICORR 2005.*, pages 103–108, June 2005.
- [22] James S. Sulzer, Michael A. Peshkin, and James L. Patton. *Design of a mobile, inexpensive device for upper extremity rehabilitation at home*, pages 933–937. 12 2007.
- [23] D. Surdilovic, R. Bernhardt, T. Schmidt, and J. Zhang. String-man: A new wire robotic system for gait rehabilitation. pages 64–67, 2003.
- [24] Salisbury Eberman Levin, Daniel E, Historical Perspective, and State Of. Raibert, m. h., "legged robots that balance." cambridge, mass.: Mit press (1986)., 1995.

-
- [25] L. C. Hsu, W. W. Wang, G. D. Lee, Y. W. Liao, L. C. Fu, and J. S. Lai. A gravity compensation-based upper limb rehabilitation robot. In *2012 American Control Conference (ACC)*, pages 4819–4824, June 2012.
- [26] G. B. Prange, A. H. A. Stienen, M. J. A. Jannink, H. van der Kooij, M. J. IJzerman, and H. J. Hermens. Increased range of motion and decreased muscle activity during maximal reach with gravity compensation in stroke patients. In *2007 IEEE 10th International Conference on Rehabilitation Robotics*, pages 467–471, June 2007.
- [27] R. J. Sanchez, J. Liu, S. Rao, P. Shah, R. Smith, T. Rahman, S. C. Cramer, J. E. Bobrow, and D. J. Reinkensmeyer. Automating arm movement training following severe stroke: Functional exercises with quantitative feedback in a gravity-reduced environment. *IEEE Transactions on Neural Systems and Rehabilitation Engineering*, 14(3):378–389, Sept 2006.
- [28] MathWorks. `fminsearch.m`, documentation.
- [29] Paolo de Leva. Adjustments to zatsiorsky-seluyanov’s segment inertia parameters. *Journal of Biomechanics*, 29(9).